

1

2 **Aminostratigraphical test of the East European Mammal Zonation for the Late Neogene and**
3 **Quaternary**

4

5 Alexey S. Tesakov^a, Pavel D. Frolov^a, Vadim V. Titov^b, Marc Dickinson^c, Tom Meijer^d, Simon A.
6 Parfitt^{e,f}, Richard C. Preece^g, Kirsty E.H. Penkman^{c*}

7

8 ^a Geological Institute, Russian Academy of Sciences, Pyzhevsky lane, 7, Moscow, Russia, 119017

9 ^b Southern Scientific Centre, Russian Academy of Sciences, Chekhov str., 41, Rostov-on-Don, Russia,
10 344006

11 ^c Department of Chemistry, University of York, York YO10 5DD, UK.

12 ^d Cainozoic Mollusca, Netherlands Centre for Biodiversity, Naturalis, P.O. Box 9517, 2300 RA Leiden,
13 The Netherlands

14 ^e Institute of Archaeology, University College London, 31-34 Gordon Square, London WC1H 0PY, UK

15 ^f Department of Earth Sciences, The Natural History Museum, Cromwell Road, London SW7 5BD, UK

16 ^g Department of Zoology, University of Cambridge, Downing Street, Cambridge CB2 3EJ UK

17 * Corresponding author

18

19 **Keywords:** Aminostratigraphy; biostratigraphy; East European Mammal zonation; Quaternary; Pliocene;
20 Pleistocene; Azov region; Black Sea region; intra-crystalline protein decomposition (IcPD); amino acid
21 racemisation (AAR); geochronology.

22

23 *Highlights*

24

- 25 • Amino acid geochronology of bithyniid opercula independently tests the East European
26 Mammal zonation.

- 27 • *Parafossarulus* and *Bithynia* opercula have similar patterns of protein degradation.
- 28 • Reworking is evident at some sites.
- 29 • Gaps in the regional palaeontological record are identified.
- 30 • Anomalously high levels of IcPD from Tizard may result from local geothermal heating.

31

32 *Abstract*

33

34 An aminostratigraphical study was undertaken to provide an independent test of the veracity of the East
35 European Mammal zonation. This important biostratigraphical scheme was originally defined from
36 reference sites in the Azov / Black Sea region of southern Russia, but is now widely used to correlate late
37 Neogene and Quaternary sediments across much of Europe and western Asia. As well as yielding a series
38 of mammal assemblages, these reference sites, which range in age from the late Pliocene (Piacenzian ca.
39 3.0 Ma) to Late Pleistocene (0.1 Ma), also contain calcitic opercula of two genera (*Bithynia* and
40 *Parafossarulus*) of freshwater gastropod snails that are suitable for amino acid dating. The intra-
41 crystalline protein decomposition (IcPD) of four amino acids (aspartic acid, alanine, valine, and glutamic
42 acid) was analysed from the opercula of these two genera, which showed similar patterns of protein
43 degradation, allowing both to be used for aminostratigraphy. The IcPD data are consistent with the
44 relative ages inferred from the mammal biostratigraphy and also with stratigraphical hiatuses interpreted
45 from the fossil record. The temporal resolution provided by IcPD data from opercula is amino acid
46 dependent, and declines in samples older than ~2 Ma. The high variability of IcPD between opercula
47 samples at some sites suggests reworking. Anomalously high levels of IcPD in samples from the Early
48 Pleistocene site of Tizard may be due to geothermal heating from local volcanism. This study provides the
49 first large-scale application of IcPD-based aminostratigraphy for the Quaternary of continental Europe,
50 and highlights its importance in testing regional stratigraphic schemes for the Late Pliocene and the
51 Pleistocene.

52

53 *1. Introduction*

54

55 Correlation of continental sequences (which are virtually always incomplete and geographically isolated)
56 is a major problem in Quaternary research, especially for those sites beyond the range of radiocarbon
57 dating. Tephrochronology has been useful in linking sequences together, but this cannot be used
58 universally, for example in regions beyond the distal outfall of tephra or for several critical periods when
59 volcanoes were inactive (Lowe *et al.*, 2015). The lack of dating methods that can cover the whole of the
60 Quaternary time period has meant that biostratigraphy has been the main technique used for correlation of
61 continental sequences. Pollen analysis has traditionally been the primary biostratigraphical technique, able
62 to discriminate some temperate stages of the Pleistocene, thereby providing differentiation of the
63 intervening cold stages. Pollen analysis underpinned the stratigraphical succession developed for The
64 Netherlands that has since become the standard template for much of NW Europe (Zagwijn, 1985). Other
65 biostratigraphical schemes are based on other biotic groups, especially mammals. During the Quaternary,
66 faunal turnover in mammalian species was relatively high, making them particularly useful for
67 biostratigraphy (Gromov, 1948; Kretzoi, 1987; Fejfar *et al.*, 1997; 1998; Mayhew, 2015; and many
68 others). Several zonation schemes have been proposed that are founded on the changing composition of
69 mammalian assemblages in response to climate and on the evolutionary trends within key lineages of
70 arvicoline rodents, such as grass voles (*Allophaiomys/Microtus*), water voles (*Mimomys/Arvicola*) and
71 steppe lemmings (*Borsodia/Prolagurus/Lagurus*). The best known, and most widely used, scheme is the
72 European Land Mammal Ages, now integrated with the Neogene MN zonation (Mein, 1990; Fejfar *et al.*,
73 1998). Combined with regional geological contexts and any possible external age control and calibration
74 points, this has enabled stratigraphical schemes to be constructed for large regions and continents (e.g.,
75 Bell *et al.*, 2004; Cione and Tonni, 2005; Nomade *et al.*, 2014, Flynn and Wu, 2017).

76

77 Several independent mammal-based Quaternary chronologies have been developed for western and

78 central Europe (e.g., Guérin, 1982; Horáček and Ložek, 1988; Rook and Martínez-Navarro, 2010). One
79 of the richest regional records of fossil mammals, including arvicoline rodents, is known in the south of
80 eastern Europe (Alexandrova, 1976; Alexeeva, 1977, 1990; Markova, 1982, 1990, 2007; Topachevsky *et*
81 *al.*, 1987, 1998; Rekovets and Nadachowski, 1995; Bajgusheva *et al.*, 2001; Nesin and Nadachowski,
82 2001; Tesakov, 2004; Titov, 2008; Agajanian, 2009, Markova and Vislobokova, 2016; and many others).
83 The Pliocene and Pleistocene sequences from the Sea of Azov region and neighbouring areas, including
84 margins of the Black Sea, North Caucasus and the lower catchment of the Don River, are particularly
85 important (Fig. 1). Continental deposits of different origin (fluvial, lagoonal, loess-paleosol) can be dated
86 by the evolutionary stage in various lineages including *Archidiskodon/Mammuthus*, *Equus*
87 (*Allohippus*)/*Equus* (*Equus*), *Arvernoceros/Megaloceros*, *Eucladoceros/Praemegaceros*,
88 *Paracamelus/Camelus*, *Allophaiomys/Microtus*, *Mimomys/Arvicola* and *Borsodia/Prolagurus/Lagurus*.
89 The chronological framework for the region in question is currently based on biostratigraphy,
90 lithostratigraphy, and paleomagnetism. One of traditional approaches is the use of small mammal
91 assemblages based on reference faunas and first appearance events (e.g., Markova, 2007; Markova and
92 Vislobokova, 2016). However for the Early Pleistocene this system is insufficiently detailed. An
93 important advance in refining the regional stratigraphy was the establishment of the MQR/MNR mammal
94 zonation for the Plio-Pleistocene of southern East Europe and western Asia. This was based on the
95 consistent application of concurrent range zones for several rapidly-evolving phyletic lineages of
96 arvicoline rodents (Vangengeim *et al.*, 2001; Tesakov, 2004; Tesakov *et al.*, 2007a). Fourteen zones were
97 defined in the Quaternary (three MNR units for the Gelasian and 11 MQR units for the rest of Quaternary,
98 ca. 2.6 Ma to Recent (Fig. 1). This East European Mammal zonation has since been applied to other
99 regions including the Ponto-Caspian (Krijgsman *et al.*, 2019), the Southern Caucasus (Tesakov, 2016;
100 Tesakov *et al.*, 2019a), Lower Volga (Zastrozhnov *et al.*, 2018), Urals (Borodin *et al.*, 2019), Anatolia
101 (van den Hoek Ostende *et al.*, 2015), central Europe (Mayhew, 2012) and as far west as the Netherlands
102 and Britain (Mayhew, 2015, Preece *et al.*, 2020).

104 Figure 1. Biostratigraphical chart of south-eastern Europe based on mammals (adapted from Tesakov *et al.*, 2017, 2019b); taxonomy of
105 *Archidiskodon/Mammuthus meridionalis* follows Baygusheva and Titov (2012).

106

107 Biostratigraphy has been successful for establishing a regional succession, but correlation between regions
108 can be problematic because migrational events can be diachronous (Walsh, 1998). It is also limited by the
109 ranges and preservation of critical species, which are not always represented in the fragmentary
110 continental fossil record. In Europe, the Early Pleistocene is an important time period for early human
111 evolution, and it is essential that a reliable chronology is developed for this period. A robust chronology
112 needs external dating and cross-checking. Attempts to test this mammalian biostratigraphy using
113 radiometric and luminescence dating are ongoing, but challenging due to temporal constraints of the
114 methods and absence of volcanic deposits throughout the region. In this study we use the developments in
115 amino acid geochronology from the intra-crystalline fraction of molluscan opercula to test the robustness
116 of the East European Mammal Zonation.

117

118 The advances in intra-crystalline preparative methods (Penkman *et al.*, 2008) and choice of material for
119 analysis (Penkman *et al.*, 2007, 2010) have improved the precision and accuracy in amino acid
120 geochronology, providing relative age estimates that extend far beyond the limits of current radiocarbon,
121 U-series and luminescence timescales. The calcite opercula of the bithyniid freshwater snails are an
122 excellent repository for the original protein, providing an intra-crystalline closed system that is better
123 protected from post-depositional environmental contamination other than mineral diagenesis. The
124 measurement of opercula intra-crystalline protein degradation (IcPD) has become an inexpensive and
125 rapid method for establishing a robust relative chronology that can be calibrated against sites of known
126 age (Penkman *et al.*, 2011, 2013).

127

128 The presence of bithyniid opercula from the same reference sites on which the East European Mammal
129 zonation of the Black Sea and Azov Sea regions was defined provides an opportunity to test the veracity
130 of this scheme. In this paper, we develop an aminostratigraphy for the Sea of Azov region using two
131 genera (*Parafossarulus* and *Bithynia*) of freshwater gastropod snails from the family Bithyniidae that have

132 calcitic opercula.

133

134 *2. Materials and methods*

135 Bithyniids are common freshwater gastropods that inhabit a wide variety of habitats. *Parafossarulus* can

136 be separated from *Bithynia* by its larger size, well-developed spiral sculpture and differences in the

137 opercula (Annandale, 1924), which have a concentric form in *Bithynia* but are paucispiral in

138 *Parafossarulus* (Girotti, 1972; Meijer, 1974; Zatravkin *et al.*, 1989; Sanko, 2007, see Fig. 2). This generic

139 distinction has recently been supported by molecular phylogenetic data (Wilke *et al.*, 2013). In Europe,

140 *Bithynia* is still extant, but *Parafossarulus* became extinct during the Middle Pleistocene, ~ 400 ka

141 (Meijer, 1974; 1986; 1989; Preece, 1990; Gittenberger *et al.*, 1998; Sanko, 2007; Lewis *et al.*, 2004).

142 *Parafossarulus* still inhabits eastern Asia, where its distribution suggests that it possibly has a greater

143 affinity for warmer environments than *Bithynia*. In most Early and early Middle Pleistocene localities in

144 the Azov region both genera occur. The extinction of *Parafossarulus* in Europe may be related to the

145 specific features of the 100 ka climatic cyclicity period and the more extreme minimum temperatures

146 attained during the glacial periods.



147

148 Figure 2. Opercula of *Bithynia* (1), with a concentric form, and *Parafossarulus* (2), which is paucispiral.
149 Scale bar equals 1 mm.
150

151 Ninety-five opercula from *Parafossarulus* and *Bithynia* were selected from 26 horizons at 16 sites (Table
152 1) that have also yielded mammal remains that enable them to be directly linked to the mammal
153 assemblage zones of the regional biostratigraphy (Vangengeim *et al.*, 2001; Tesakov *et al.*, 2007a). Most
154 of the fossil localities are situated along the shores of the Taganrog Gulf of the Sea of Azov, the lower
155 catchment of the Don River, and the western part of North Caucasus including the Taman Peninsula (Fig.
156 3). Material from multi-layered Early Pleistocene locality Kryzhanovka (SW Ukraine) came from the
157 lower, Gelasian, part of the section (Tesakov, 2004), not to be confused with the well-known upper bed of
158 Kryzhanovka correlated with the Gelasian-Calabrian transition (Rekovets, Nadachowski, 1995). The Port-
159 Katon 4 locality (Tesakov *et al.*, 2007), of mid Middle Pleistocene age, is much younger than the well-
160 known Early Pleistocene site of Port-Katon (Markova, 1982, 1990). The opercula, collected between
161 1988 and 2018, were mostly extracted in the field, but some sediment samples needed hot water for
162 disaggregation in the laboratory. Heating increases amino acid D/L values, but the duration of the hot
163 water disaggregation (opercula would only have experienced heating > 40°C for less than 30 minutes)
164 would not have been sufficient to alter the D/L values. Samples were stored at the Geological Institute
165 RAS (Moscow) and Southern Scientific Centre RAS (Rostov-on-Don) before transfer to the University of
166 York for amino acid analysis.

167 To establish the IcPD behaviour of *Bithynia* and *Parafossarulus*, we also analysed 11 opercula from two
168 additional sites outside the main study region where both genera co-occur. These sites are Korotoyak V7
169 (=Korotoyak 3a, Uspenka Suite, Early Pleistocene, not to be confused with a slightly younger Early
170 Pleistocene site of Korotoyak 3c, Ostragozh Suite described by Markova, 2005) in the upper catchment of
171 the Don River (Iossifova and Semenov, 1998; Agajanian, 2009) and the Tiglian type-site at Tegelen, the
172 Netherlands (Freudenthal *et al.*, 1976; Penkman *et al.*, 2013).

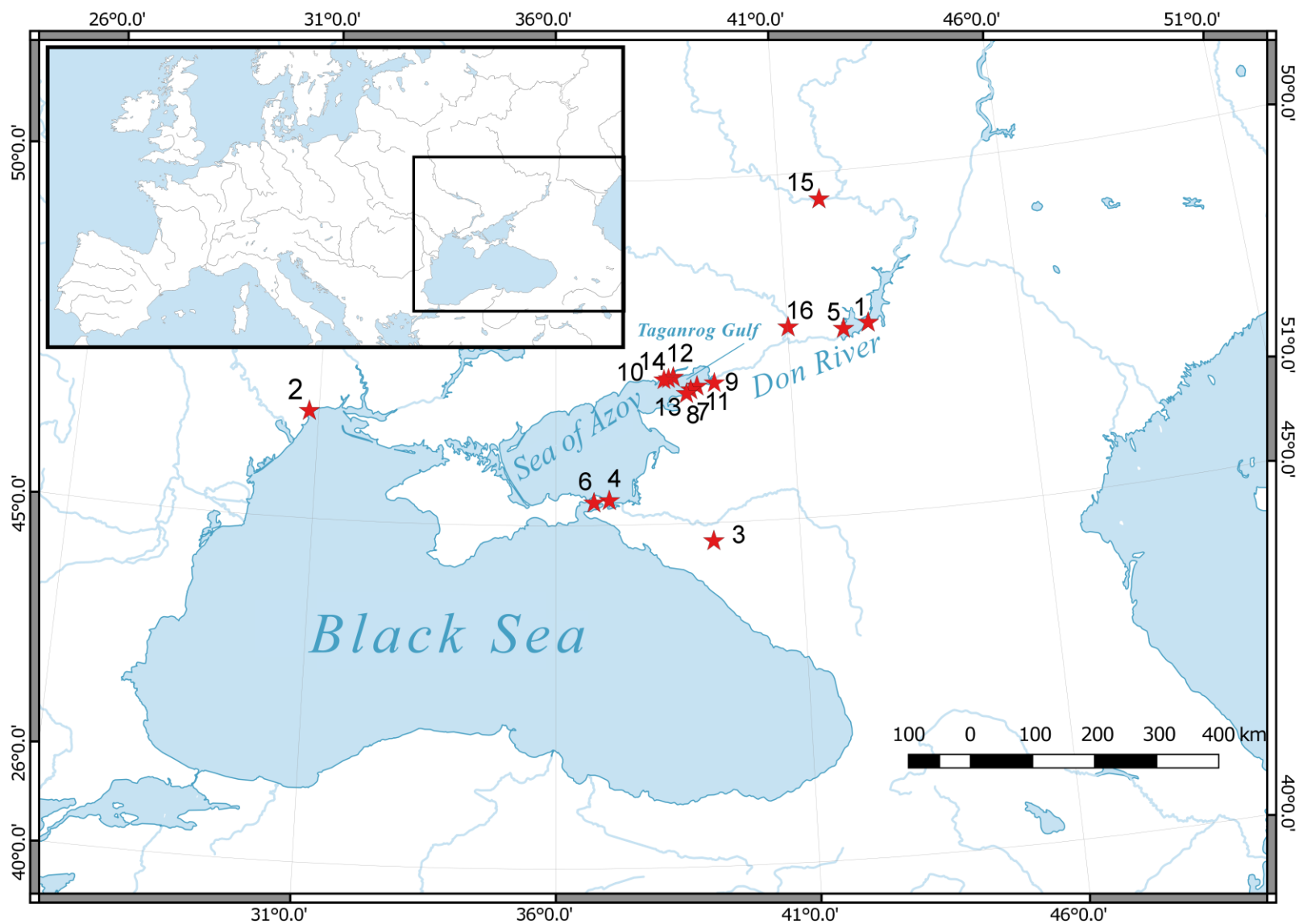
Locality Number and code	Site & reference	Geographical location	Chronostratigraphy	MQR/MNR	Age range estimate, Ma	Genus	n
1. Krv	Krivsky [Chegis <i>et al.</i> , 2017]	Lower Don River	Late Pliocene, Piacenzian	MNR5	>2.5	<i>Parafossarulus</i>	4
2. Kr2	Kryzhanovka 2 [Tesakov, 2004]	NW Black Sea coast, Ukraine	early Early Pleistocene, Gelasian	MNR3	ca. 2.4	<i>Parafossarulus</i>	3
2. Kr3	Kryzhanovka 3 [Tesakov, 2004]	NW Black Sea coast, Ukraine	Early Pleistocene, Gelasian	MNR2	2.2-2.3	<i>Parafossarulus</i>	4
3. Psk	Psekups [Tesakov, 2004]	North Caucasus	Early Pleistocene, Gelasian	MNR1	2.1-2.2	<i>Bithynia</i>	3
4. Tz1	Tizdar 1 [Tesakov, 2004]	Taman Peninsula	Early Pleistocene, Gelasian-Calabrian transition	MQR11	2.0-2.1	<i>Bithynia</i>	4
4. Tz1	Tizdar 1 [Tesakov, 2004]	Taman Peninsula	Early Pleistocene, Gelasian-Calabrian transition	MQR11	2.0-2.1	<i>Parafossarulus</i>	4

4. TzK	Tizdar K [Shchelinsky <i>et al.</i> , 2016]	Taman Peninsula	Early Pleistocene, Gelasian-Calabrian transition	MQR10	1.6-2.0	<i>Bithynia</i>	4
4. Tz2	Tizdar 2 [Tesakov, 2004]	Taman Peninsula	Early Pleistocene, Gelasian-Calabrian transition	MQR10	1.6-2.0	<i>Bithynia</i>	4
4. Tz2	Tizdar 2 [Tesakov, 2004]	Taman Peninsula	Early Pleistocene, Gelasian-Calabrian transition	MQR10	1.6-2.0	<i>Parafossarulus</i>	3
5. Srk	Sarkel [Dodonov <i>et al.</i> , 2007; Nikolskiy <i>et al.</i> , 2014]	Lower Don River	Early Pleistocene, Gelasian-Calabrian transition	MQR8	1.0-1.2	<i>Bithynia</i>	4
6. MaK	Malyi Kut [Pilipenko <i>et al.</i> , 2015, and new data]	Taman Peninsula	Calabrian, late Early Pleistocene	MQR7-8	0.9-1.0	<i>Parafossarulus</i>	2
7. Se1	Semibalki 1 [Tesakov <i>et al.</i> , 2007b]	Taganrog Gulf	Calabrian, late Early Pleistocene	MQR7	0.8-1.0	<i>Bithynia</i>	4
7. Se1	Semibalki 1 [Tesakov	Taganrog Gulf	Calabrian, late Early	MQR7	0.8-1.0	<i>Parafossarulus</i>	4

	<i>et al.</i> , 2007b]		Pleistocene				
8. Mg2	Margaritovo 2 [Tesakov <i>et al.</i> , 2007b]	Taganrog Gulf	Calabrian, late Early Pleistocene	MQR7	0.8-1.0	<i>Bithynia</i>	4
8. Mg2	Margaritovo 2 [Tesakov <i>et al.</i> , 2007b]	Taganrog Gulf	Calabrian, Early Pleistocene	MQR7	0.8-1.0	<i>Parafossarulus</i>	4
9. Zel	Zelenyi [new data]	Taganrog Gulf	early Middle Pleistocene	MQR4-6	0.5-0.7	<i>Bithynia</i>	4
9. Zel	Zelenyi [new data]	Taganrog Gulf	early Middle Pleistocene	MQR4-6	0.5-0.7	<i>Parafossarulus</i>	3
7. Se2	Semibalki 2 [Tesakov <i>et al.</i> , 2007b]	Taganrog Gulf	early Middle Pleistocene	MQR4-6	0.5-0.7	<i>Parafossarulus</i>	4
10. Pla	Platovo [Tesakov <i>et al.</i> , 2007b]	Taganrog Gulf	early Middle Pleistocene	MQR4-6	0.5-0.7	<i>Parafossarulus</i>	3
11. Stf	Stefanidinodar [new data]	Taganrog Gulf	early Middle Pleistocene	MQR4-6	0.5-0.7	<i>Bithynia</i>	4

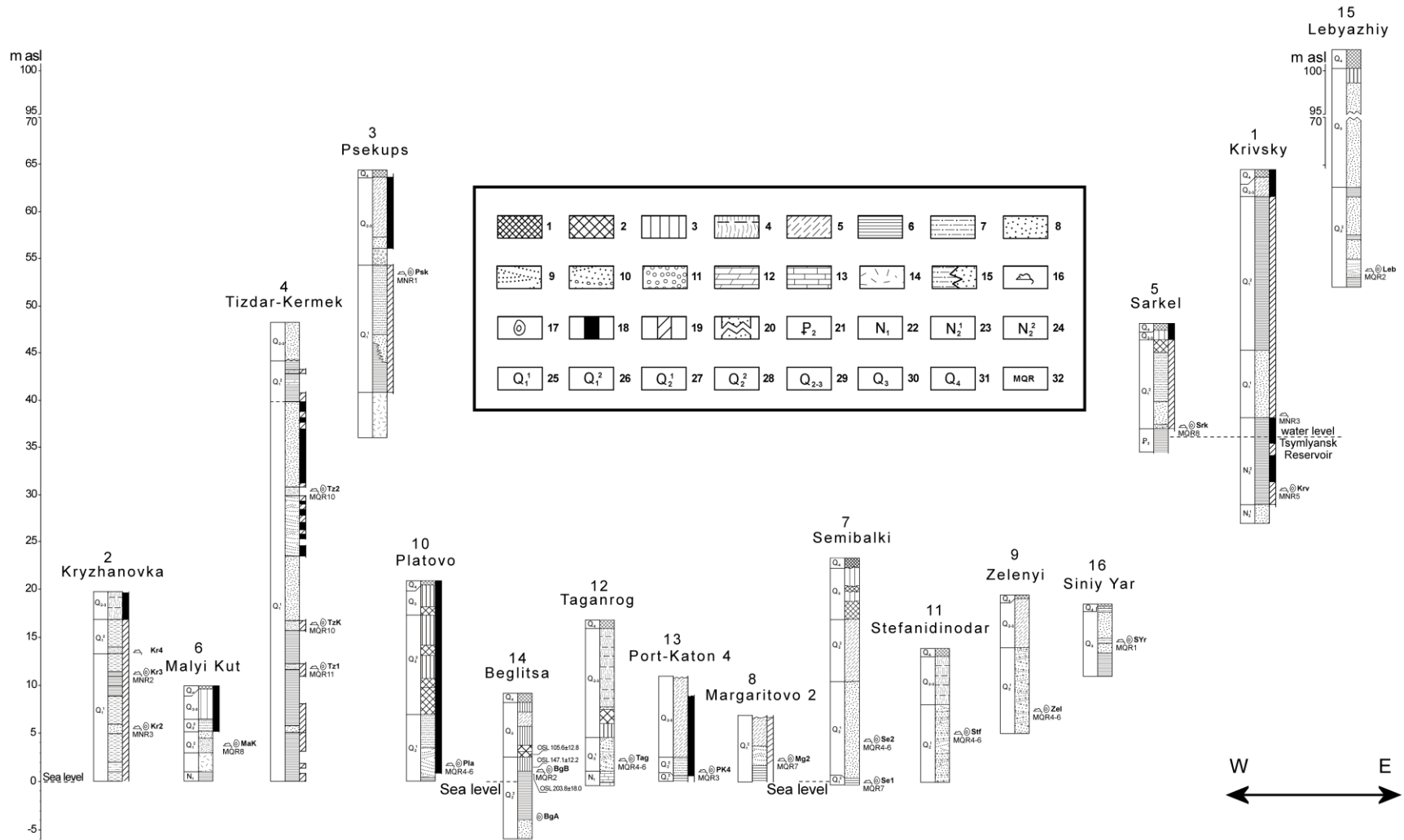
12. Tag	Taganrog [new data]	Taganrog Gulf	early Middle Pleistocene	MQR4-6	0.5-0.7	<i>Parafossarulus</i>	4
13. PK4	Port-Katon 4 [Tesakov <i>et al.</i> , 2007b]	Taganrog Gulf	early Middle Pleistocene	MQR3	0.3-0.5	<i>Parafossarulus</i>	4
14. BgA	Beglitsa A core [new data]	Taganrog Gulf	late Middle Pleistocene	MQR2	0.2-0.3	<i>Bithynia</i>	2
14. BgB	Beglitsa B [Tesakov <i>et al.</i> , 2007b]	Taganrog Gulf	late Middle Pleistocene	MQR2	0.2-0.3	<i>Bithynia</i>	4
15. Leb	Lebyazhiy (=Veshenskaya) [Baygusheva <i>et al.</i> , 2014]	Lower Don River	late Middle Pleistocene	MQR2	0.2-0.3	<i>Bithynia</i>	4
16. SYr	Siniy Yar ‘ [Tesakov <i>et al.</i> , 2012]	Lower Don River	Late Pleistocene	MQR1	0-0.1	<i>Bithynia</i>	4
17. Ky7	Korotoyak V7 [= Korotoyak 3a in Iossifova and	Upper Don River	late Early Pleistocene	MQR8	1.0-1.2	<i>Bithynia</i>	4

	Semenov, 1998; = Korotoyak 3 in Agajanian, 2009]						
17. Ky7	Korotoyak V7 [= Korotoyak 3a in Iossifova and Semenov, 1998; = Korotoyak 3 in Agajanian, 2009]	Upper Don River	late Early Pleistocene	MQR8	1.0-1.2	<i>Parafossarulus</i>	2
18. Teg	Tegelen [Freudenthal <i>et al.</i> , 1976; Penkman <i>et al.</i> , 2013]	Netherlands	Early Pleistocene, Gelasian	MNR1	2.1-2.2	<i>Bithynia</i>	4
18. Teg	Tegelen [Freudenthal <i>et al.</i> , 1976; Penkman <i>et al.</i> , 2013]	Netherlands	Early Pleistocene, Gelasian	MNR1	2.1-2.2	<i>Parafossarulus</i>	4



175

176 Figure 3. Map of the fossil sites in the Azov region. 1. Krivsky, 2-3. Kryzhanovka 2 and 3, 4.Psekups, 4.Tizdar, 5. Sarkel, 6. Malyi Kut, 7.
 177 Semibalki 1 and 2, 8. Margaritovo 2, 9. Zelenyi, 10. Platovo, 11. Stefanidinodar, 12. Taganrog, 13. Port-Katon 4, 14. Beglitsa, 15. Lebyzhiy, 16.



179
 180 Figure 4. Schematic geological sections of the localities studied with the elevation above sea level (m). 1. Modern soil. 2. Palaeosol. 3. Loess. 4.
 181 Loess-palaeosol sequence. 5. Subaerial loam. 6. Clay. 7. Sandy clay. 8. Sand. 9. Cross-bedded sand. 10. Gravel. 11. Pebbles. 12. Marl. 13.
 182 Limestone. 14. Talus. 15. Facies boundaries. 16. Mammal remains relevant to biostratigraphy. 17. Opercula sampled in this study. 18. Normal
 183 palaeomagnetic polarity. 19. Reversed polarity. 20. Thickness not to scale. 21. Eocene. 22. Miocene. 23. Early Pliocene. 24. Late Pliocene. 25.
 184 Early Pleistocene (Gelasian). 26. Early Pleistocene (Calabrian). 27. early Middle Pleistocene. 28. late Middle Pleistocene. 29. Middle-Late

185 Pleistocene. 30. Late Pleistocene. 31. Holocene. 32. Biostratigraphical zones. Data from Baygusheva *et al.*, 2014; Chegis *et al.*, 2017; Chen *et al.*,
186 2018; Dodonov *et al.*, 2007; Pilipenko *et al.*, 2015; Shchelinsky *et al.*, 2016; Tesakov, 2004; Tesakov *et al.*, 2007b, 2012, 2019b. Numbers above
187 section names match site numbers in Figure 3.
188

189

190 All samples were prepared using the procedures of Penkman *et al.* (2008) to isolate the intra-crystalline
191 protein by bleaching. In brief, two subsamples were then taken from each operculum; one fraction was
192 directly demineralised and the free amino acids analysed (referred to as the 'free' amino acids, FAA), and
193 the second was hydrolysed at 110°C for 24 hours to release the peptide-bound amino acids, thus yielding
194 the 'total' amino acid concentration, referred to as the 'total hydrolysable amino acid fraction (THAA).
195 Samples were analysed in duplicate by RP-HPLC, with standards and blanks run alongside samples.
196 During hydrolysis, both asparagine and glutamine undergo rapid irreversible deamination to aspartic acid
197 and glutamic acid, respectively (Hill, 1965). It is therefore not possible to distinguish between the acidic
198 amino acids and their derivatives and they are reported together as Asx and Glx, respectively.

199

200 The D/L values of aspartic acid/asparagine, glutamic acid/glutamine, serine, alanine and valine (D/L Asx,
201 Glx, Ser, Ala, Val) and the concentrations of Ser and Ala ([Ser]/[Ala]) were then assessed to provide an
202 overall estimate of intra-crystalline protein decomposition (IcPD). These amino acids are the best
203 chromatographically resolved enantiomer pairs for opercula (Powell *et al.*, 2013), and between them also
204 cover a wide temporal range (Penkman *et al.*, 2011). In a closed system, the amino acid ratios of the FAA
205 and the THAA subsamples should be highly correlated, enabling the recognition of compromised samples
206 (e.g., Preece and Penkman, 2005). The D/L of an amino acid will increase with increasing time, whilst the
207 [Ser]/[Ala] value will decrease. Each amino acid racemises at different rates, and therefore is useful over
208 different timescales. The D/L of Ser is less useful as a geochronological tool as its breakdown patterns
209 mean that a single D/L value can represent more than one time-point in samples of this age. However,
210 D/L Ser is reported here as aberrant values are useful indications of contamination (e.g. Williams and
211 Smith, 1977; Kosnik and Kaufman, 2008).

212

213 *3. Results and Discussion*

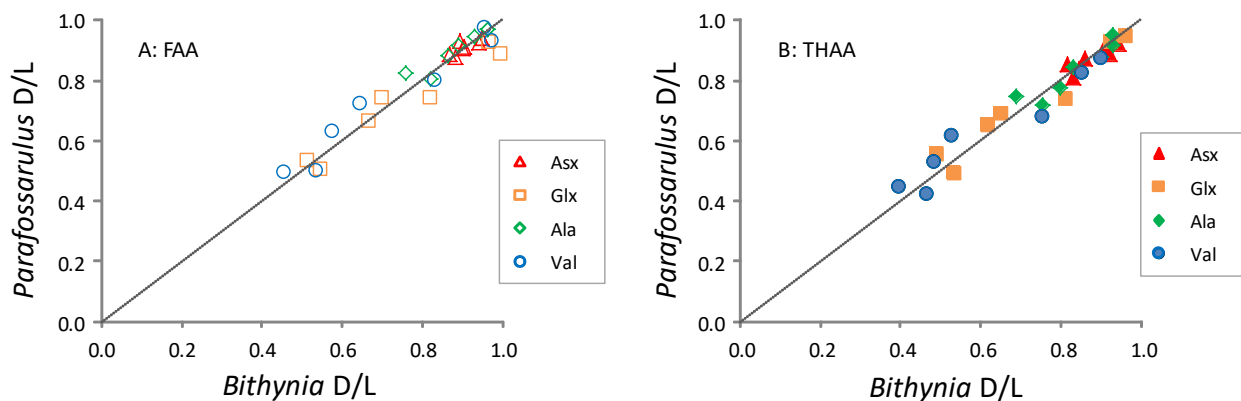
214

215 **3.1 Comparison of D/L values in co-occurring *Parafossarulus* and *Bithynia***

216 Five Russian sites yielded *Bithynia* and *Parafossarulus* opercula from the same horizons: two from the
217 Taman Peninsula (Tizard 2, Tizard 1) and three from the margins of the Taganrog Gulf (Margaritovo 2,
218 Semibalki 1, Zelenyi). IcPD data from these have been compared with data from Korotoyak V7 (Upper
219 Don region) and previously published data from the type-site of the Tiglian (Penkman *et al.*, 2011; 2013).

220

221



222

223 Fig. 5: Comparison of mean D/L values of *Parafossarulus* and *Bithynia* for (A) the free amino acids
224 (FAA) and (B) the total hydrolysable amino acids (THAA) Asx, Glx, Ala and Val from the Azov sites
225 Tizard 1, Tizard 2, Margaritovo 2, Semibalki 1 and Zelenyi, the Lower Don site Korotoyak and the
226 Tiglian type-site at Tegelen; the grey line indicates a 1:1 relationship.
227

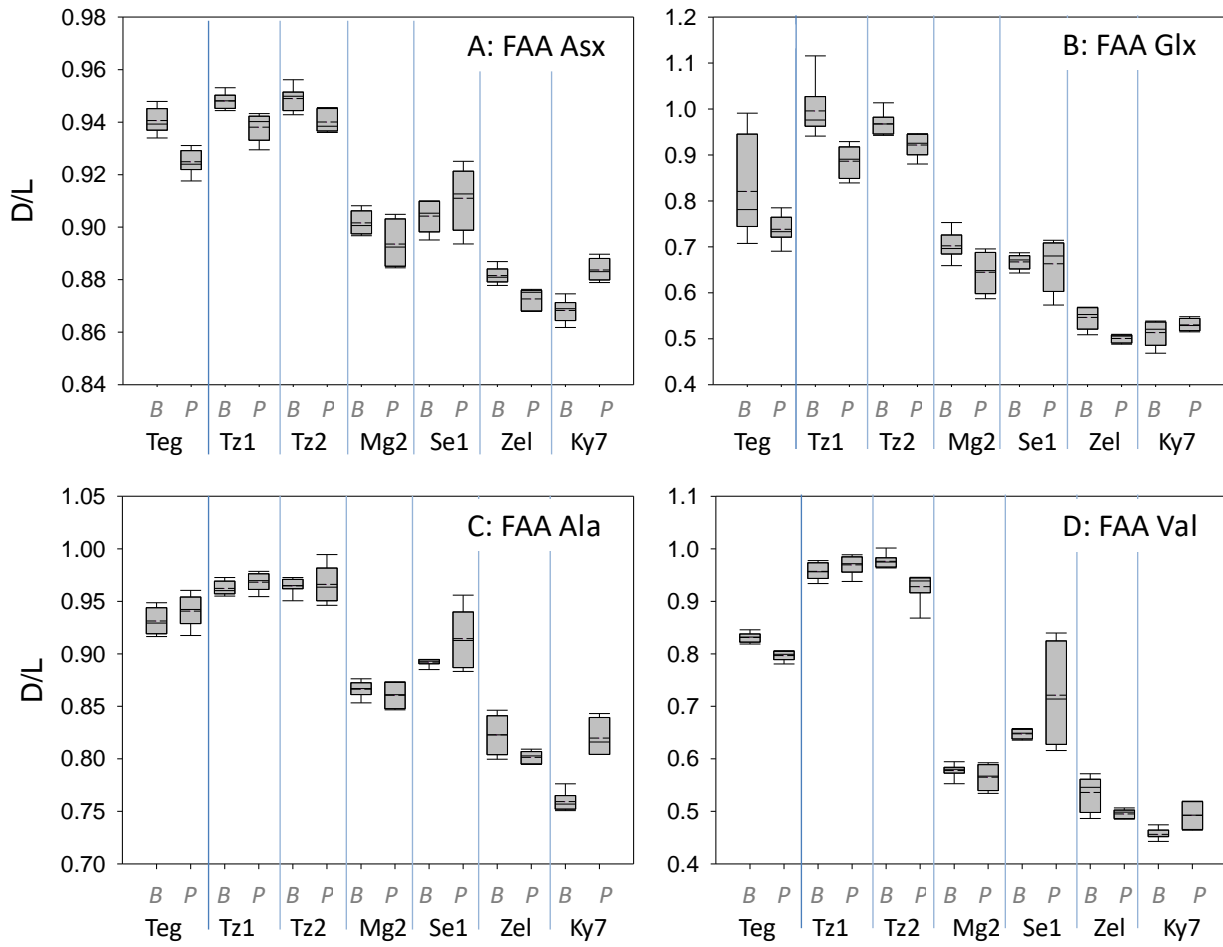
228 There is a strong correlation between the extent of racemisation in the opercula of each genera from the
229 same horizons (Fig. 5). A Student's 2-tailed t-test (or Mann-Whitney for data that was not normal), which
230 assesses the probability that the two samples are derived from the same population, showed that in 23
231 cases (41%) the amino acids in *Bithynia* were more racemised than in *Parafossarulus* from a site. In 14
232 cases (25%) amino acids from *Parafossarulus* were more racemised than those from *Bithynia*, and in 19
233 cases there was no significant difference (34%). There are therefore no consistent differences between the
234 racemisation of these genera from the same stratigraphical horizon (Table 2; Fig.6). Analysis of a greater
235 number of individuals per site (as well as a larger number of sites) will enable any interspecific
236 differences to be better resolved, but we conclude from the existing dataset that it is possible to make

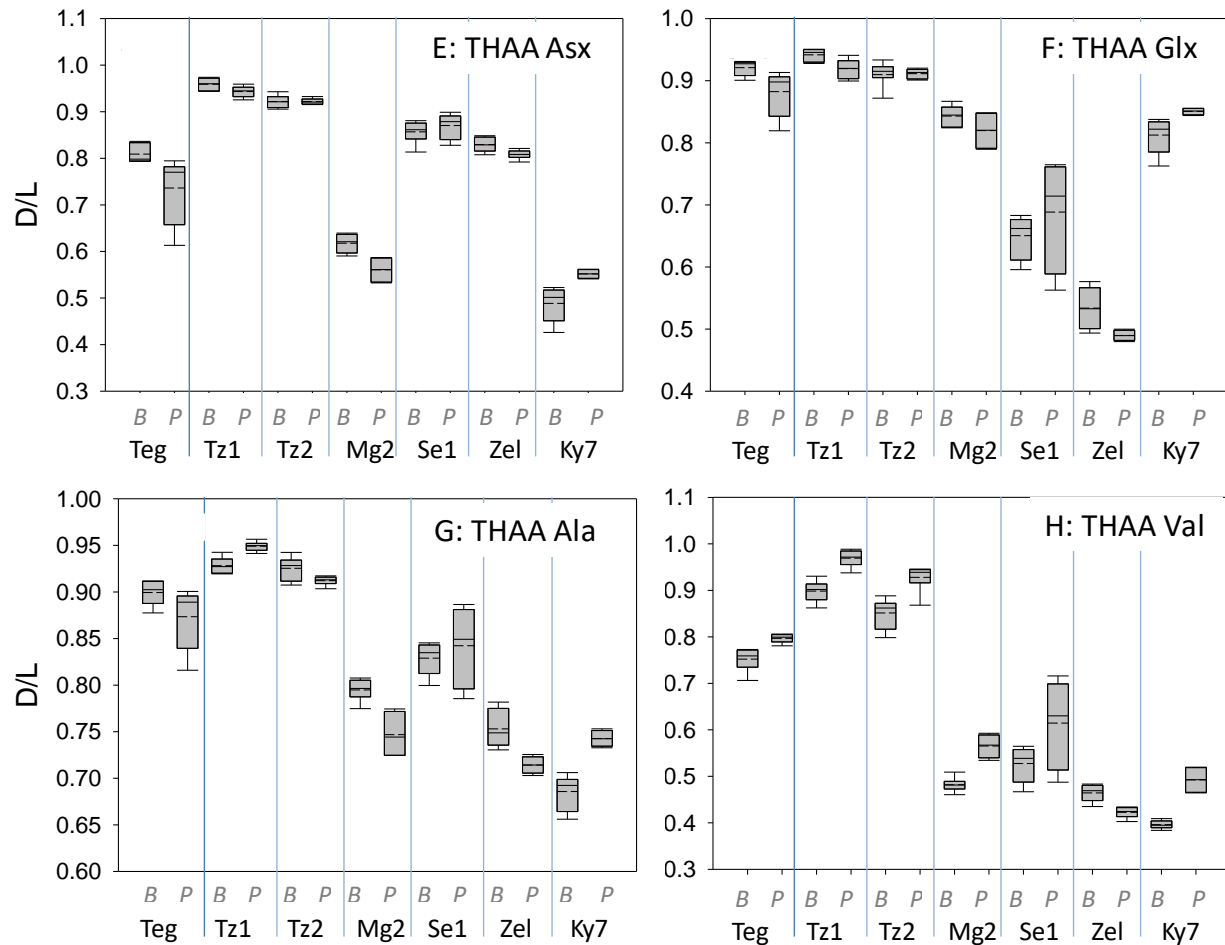
237 direct comparisons of the IcPD data from the opercula of these two genera, which can therefore be used
238 interchangeably, providing complementary data.

Site	FAA				THAA				Which genus is higher?		
	Asx	Glx	Ala	Val	Asx	Glx	Ala	Val	<i>B</i> > <i>P</i> (n)	<i>P</i> > <i>B</i> (n)	no sig. diff.
Teg	0.000 <i>B</i>	<i>0.050</i>	0.184	0.000 <i>B</i>	0.003 <i>B</i>	0.013 <i>B</i>	<i>0.108</i>	0.001 <i>P</i>	4	1	3
Tz1	0.001 <i>B</i>	0.001 <i>B</i>	0.186	0.201	0.035 <i>B</i>	0.009 <i>B</i>	0.000 <i>P</i>	0.000 <i>P</i>	4	2	2
Tz2	0.002 <i>B</i>	0.005 <i>B</i>	0.847	0.002 <i>B</i>	0.993	0.852	0.032 <i>B</i>	0.003 <i>P</i>	4	1	3
Mg2	0.068	0.024 <i>B</i>	0.364	0.267	0.004 <i>B</i>	0.115	0.001 <i>B</i>	0.000 <i>P</i>	3	1	4
Se1	0.166	0.846	0.049 <i>P</i>	0.054	<i>0.161</i>	0.272	0.423	0.029 <i>P</i>	0	2	6
Zel	0.001 <i>B</i>	0.002 <i>B</i>	0.028 <i>B</i>	0.024 <i>B</i>	0.011 <i>B</i>	0.008 <i>B</i>	0.001 <i>B</i>	0.000 <i>B</i>	8	0	0
Ky7	0.000 <i>P</i>	0.285	0.000 <i>P</i>	0.009 <i>P</i>	0.004 <i>P</i>	0.004 <i>P</i>	0.000 <i>P</i>	0.000 <i>P</i>	0	7	0
<i>B</i> > <i>P</i> (n)	4	4	1	3	4	3	3	1	23		
<i>P</i> > <i>B</i> (n)	1	0	2	1	1	1	2	6	14		
no sig. diff.	2	3	4	3	2	3	2	0	19		
%									41.1%	25.0%	33.9%

240

241 Table 2: p-values for the Student's 2-tailed t-test (for normally distributed data) and Mann-Whitney tests (for non-normal data, p-value is
242 italicised) for Asx, Glx, Ala and Val D/L in both FAA & THAA for *Parafossarulus* (*P*) and *Bithynia* (*B*) at each site: Teg = Tegelen; Tz1 = Tizdar
243 1; Tz2 = Tizdar 2; Mg2 = Margaritovo; Se1 = Semibalki 1; Zel = Zelenyi; Ky7 = Korotoyak. Bold values show that the extent of racemisation is
244 statistically different between the two genera at that site at the 95% confidence level; the genus that is higher is signified by its initial. No
245 consistent offset between the two genera is observable.





248

249

250 Figure 6: D/L of free amino acid (FAA: A, B, C & D) and total hydrolysable amino acid (THAA: E, F, G
 251 & H) intra-crystalline fractions of *Bithynia* (B) and *Parafossarulus* (P) opercula from the same horizons
 252 for the 7 sites. Site abbreviations are as in Table 2. For each sample, the box encloses the 25th and 75th
 253 percentiles. Within the box, the solid line indicates the median and the dashed line shows the mean.

254

255 Where enough data points are available, the 10th and 90th percentiles can be calculated (shown by lines
 256 below and above the boxes respectively). The results of each duplicate analysis are included in order to
 257 provide a statistically significant sample size. No consistent difference between the D/L values of *Bithynia*
 258 and *Parafossarulus* is apparent in this dataset.

259

258 3.2. D/L vs mammal zones

259

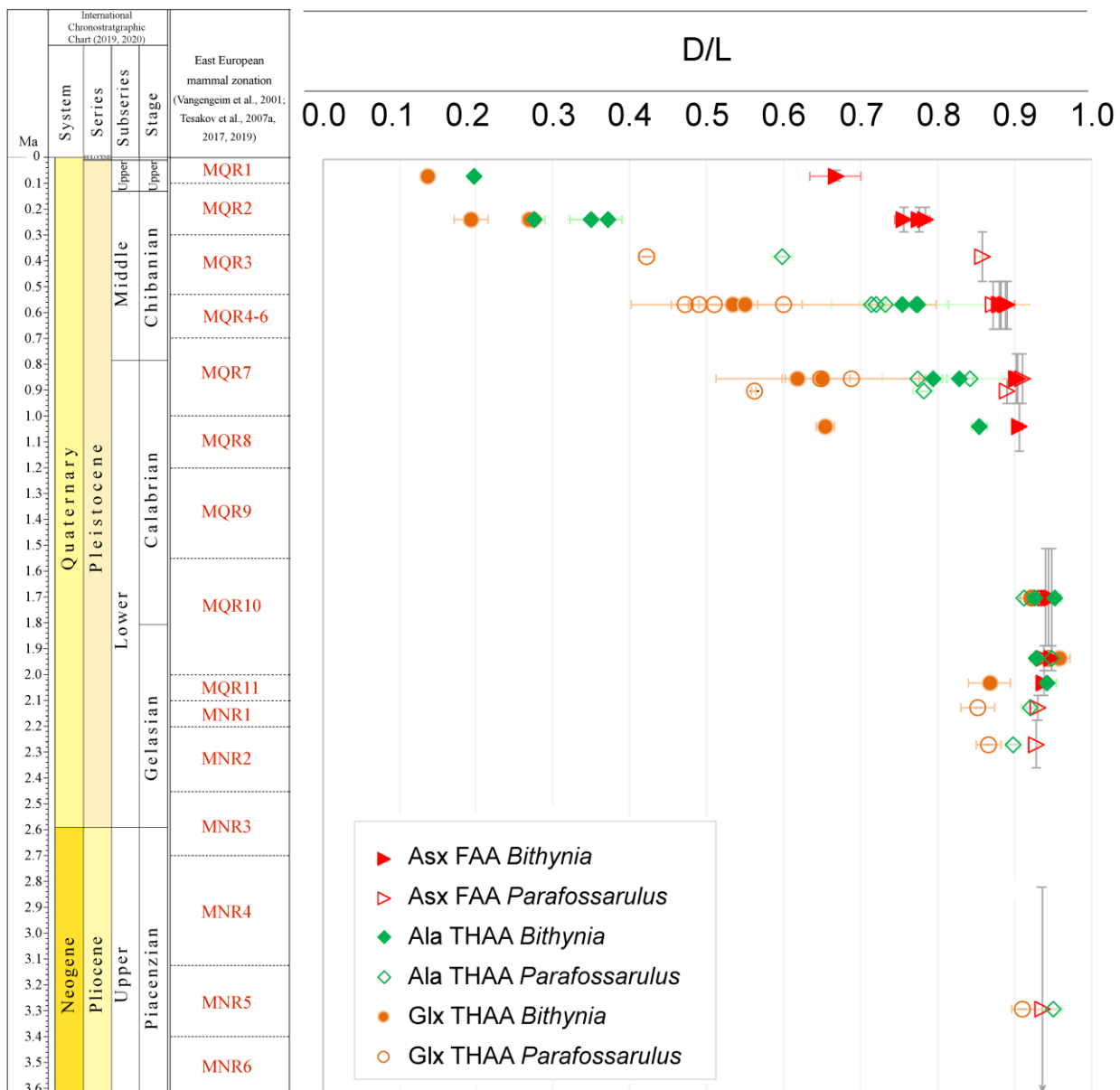
260 The Quaternary biostratigraphical chronology established in southeastern Europe on the basis of stages of
 261 mammalian evolution can be compared with the opercula IcPD (D/L values) for the four amino acids

262

263 reported: alanine (Ala), aspartic acid (Asx), glutamic acid (Glx), and valine (Val). The D/L values plotted
 264 against the MQR zonation show a generally consistent pattern of increasing racemisation in successively

265

266 older samples (Fig. 7).



264

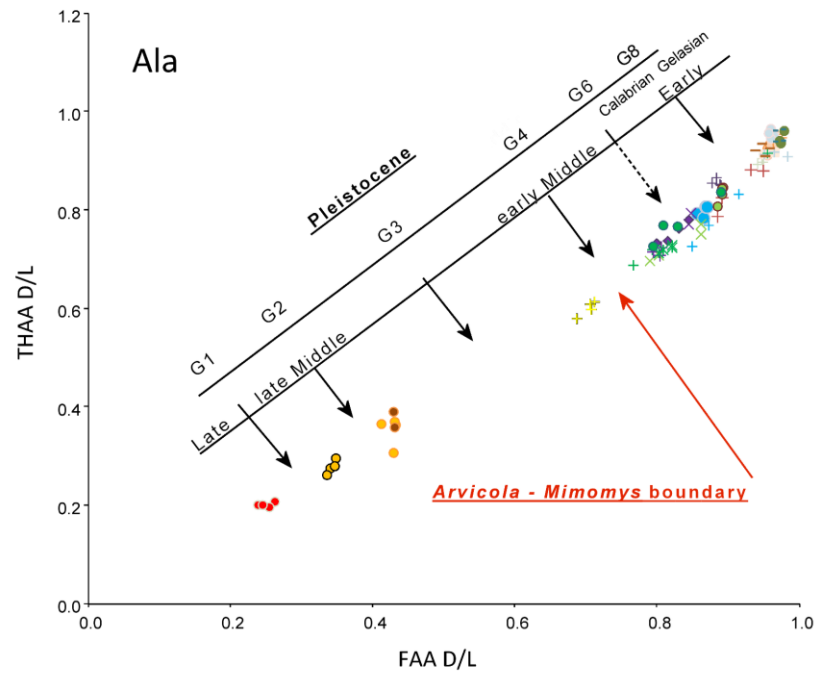
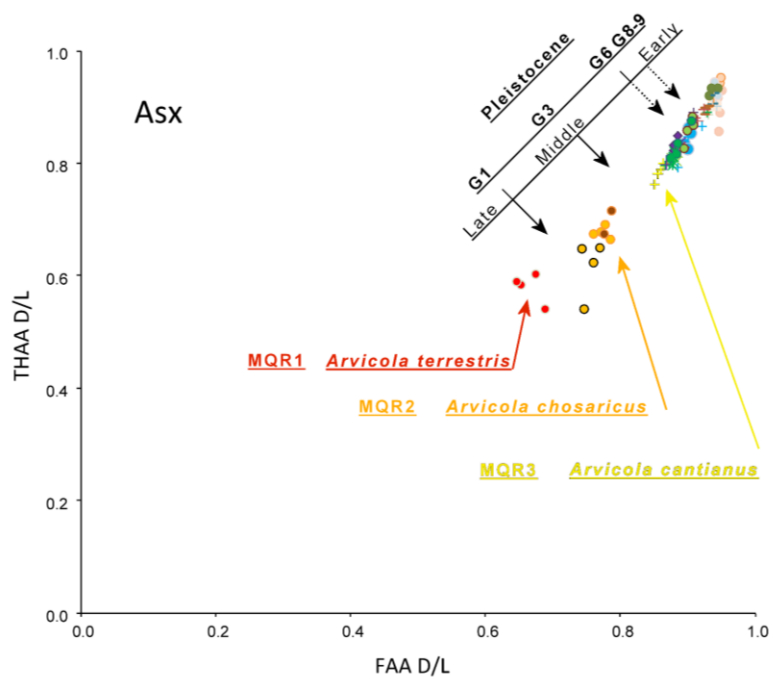
265 Figure 7. Selected mean D/L values (only FAA Asx, THAA Ala and Glx D/Ls shown for clarity) from all
 266 bithyniid opercula from each horizon plotted against the standard global MIS timescale and East
 267 European Mammal zonation. For simplicity, the x-error bars, indicating the current uncertainty on the age
 268 of the deposits, are shown for the Asx data. Y-error bars indicate two standard deviations about the mean
 269 for each site. *Bithynia* opercula are represented by closed symbols; *Parafossarulus* opercula by open
 270 symbols.

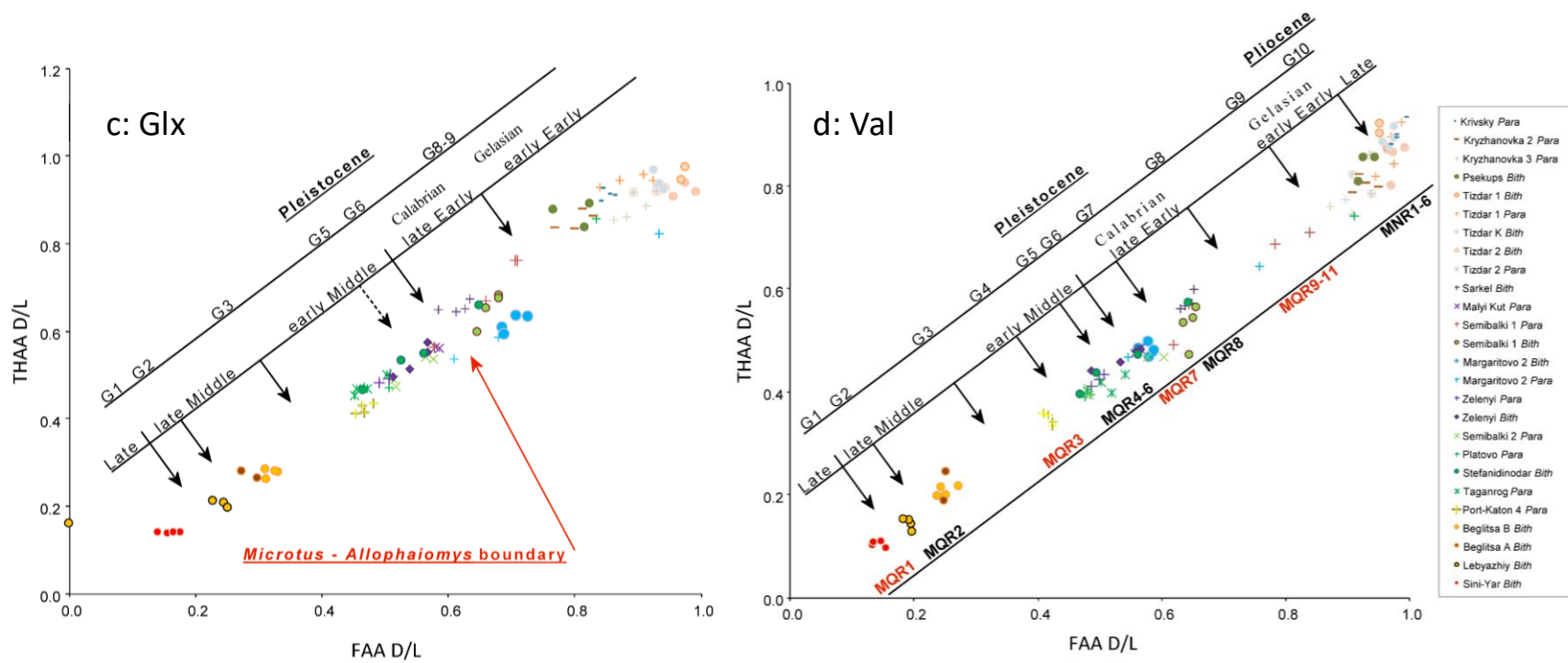
271
272 The extent of IcPD (Fig. 7) increases with increasing age and is stratigraphically consistent with the
273 mammal zonation. Amino acids with faster rates of racemisation (e.g., Asx) enable greater temporal
274 resolution in progressively younger sites, whereas the slower racemisers (e.g., Glx) provide temporal
275 information in this region over at least 2 Ma. In a few cases the D/L values have a larger range than
276 expected, which may result from non-closed system behaviour (Sec. 3.3), an effective diagenetic
277 temperature difference across the region, sites of different ages within a discrete mammal zone (Sec 3.4),
278 or reworking (Sec. 3.5).

279
280 **3.3. IcPD and closed system behaviour**

281
282 The extent of intra-crystalline protein decomposition in both the FAA and THAA fractions increases with
283 time, with the temperature dependence of the reactions resulting in increased levels of protein breakdown
284 occurring during warm stages and decreased degradation during cold stages (e.g. Miller *et al.*, 1999). Sites
285 within a small geographical area, such as those in the Azov region under discussion, can be assumed to
286 have experienced similar thermal histories, allowing the construction of a regional aminostratigraphic
287 framework on the basis that contemporary sites have similar IcPD values. Plotting FAA D/L values
288 against THAA D/L values shows a high correlation between fractions for each amino acid for the Azov
289 dataset (Figs. 8a-8d). As compromised samples would fall away from the trend (Preece and Penkman,
290 2005), this indicates that the IcPD in opercula from this region exhibit the expected closed system
291 behaviour. The high variability observed at some sites is therefore unlikely to be due to non closed
292 system behaviour in these samples.

293





295

296 Figure 8. FAA vs THAA D/Ls for (a) Asx, (b) Ala, (c) Glx and (d) Val for the intra-crystalline fraction of individual bithyniid opercula from the
 297 Azov region. High correlation between the FAA and THAA fractions indicates closed-system behaviour, providing the foundation for a robust
 298 aminostratigraphy. Diagonal axes show how the amino acid data relate to the divisions of the Pleistocene and the East European Mammal zones
 299 (MQR/MNR zonation). G1-G10 highlight potential gaps in the range of D/L values that correspond to breaks in the regional fossil record (see
 300 section 3.7). Coloured arrows indicate important biostratigraphical events.
 301

302 3.4 Aminostratigraphic resolution within a mammal I assemblage zone

303

304 Fossiliferous levels from Lebyazhiy and Beglitsa are both attributed to MQR2 (late Middle Pleistocene)
305 on the basis of mammalian biostratigraphy and supported by lithostratigraphy. The horizons analysed
306 from Beglitsa are situated below a MIS 5 palaeosol complex Eemian or Mezin paleosol complex of the
307 regional soil stratigraphy (Tesakov *et al.*, 2007b)) and the Lebyazhiy fossil bed (Baygusheva *et al.*, 2014)
308 are at the base of the third, 40-45 m terrace of the Don River terrace sequence correlated with the late
309 Middle Pleistocene (Krasnenkov and Kazantseva, 1993; Kholmovoi, 200). Both faunas contain water
310 voles with generally undifferentiated enamel (*Arvicola chosaricus*) and an early form of *Mammuthus*
311 *primigenius* (Tesakov *et al.*, 2007b; Baygusheva *et al.*, 2014). The amino acids from opercula analysed
312 from both horizons at Beglitsa (Fig. 4) are consistently more racemised than those from Lebyazhiy (Fig.
313 8), which either indicates that the Beglitsa opercula are older than those from Lebyazhiy, or that there are
314 significant temperature differences between the sites, which are ~300 km apart, Lebyazhiy being the more
315 northerly. Recent mean annual temperatures in the period of 2000-2019 recorded in the vicinities of both
316 sites differ by about 2°C: with 11.2°C for Beglitsa (meteostation of Taganrog) and 9.1°C (meteostation of
317 Serafimovich) according to the weather archive of the web project “Pogoda i klimat” (accessed May,
318 2020). The lower temperatures at Lebyazhiy might therefore produce lower IcPD values than
319 contemporary samples from warmer sites, such as Beglitsa. However the IcPD differences might possibly
320 reflect a true difference in age, with Beglitsa being slightly older than Lebyazhiy.

321 In Beglitsa, the upper horizon with opercula (Beglitsa B) occurs in fluvial to brackish water estuarine
322 deposits several metres below the Eemian (basal Late Pleistocene) soil complex. It had been assumed to
323 have been deposited relatively close in time to the Eemian, but the duration of the gap between the
324 estuarine deposits with mammals and the Eemian soil was unknown. Recent OSL dating of the Beglitsa
325 section suggests that the age of the lower horizon of the Eemian palaeosol complex (correlated with the
326 Last Interglacial, MIS 5e) is 105.6 ± 12.8 ka, the underlying sandy loess is 147.1 ± 12.2 ka, whereas the
327 basal lagoonal deposits yielding *Bithynia* opercula (Beglitsa B) is 203.8 ± 18.0 ka (Chen *et al.*, 2018), i.e. in

328 the lower part of MQR2 unit. The lower sample, Beglitsa A, comes from a borehole, 5-6 m below the
329 upper level (Beglitsa B), and shows no significant differences in IcPD from the Beglitsa B sample,
330 implying a similar age for the lagoonal deposits. Although the precise position of the fauna of Lebyazhiy
331 in the time range of MQR2 is unknown, it cannot be excluded that the two sites (Lebyazhiy and Beglitsa)
332 belong to different parts of mammal biozone MQR2 as suggested by IcPD values.

333

334 **3.5. Evidence of reworking**

335

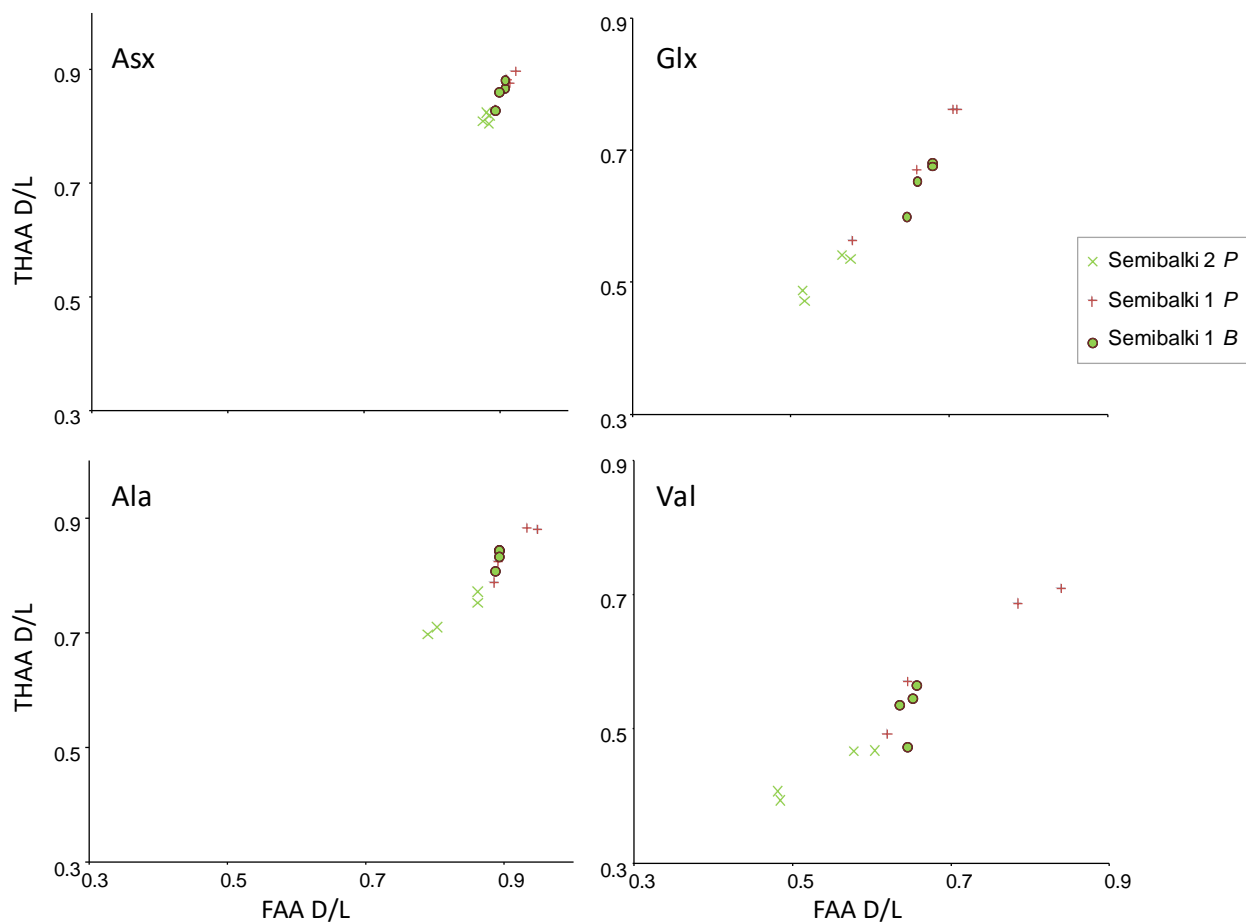
336 Bithyniid opercula from discrete horizons at Platovo (MQR 4-6), Margaritovo 2 (MQR7), Semibalki
337 (MQR 4-6 and 7) and Stefanidinodar (MQR 4-6) show a large range of IcPD values between samples,
338 with at least one outlier exhibiting much higher levels of protein breakdown. Reworking of opercula is
339 always a potential issue, because they are composed of calcite that is more stable and robust than shells
340 composed of aragonite, which are more susceptible to diagenetic loss. Moreover, their flat morphology
341 and higher density increases the likelihood of hydrodynamic sorting; indeed, the ratio of bithyniid shell to
342 opercula has been used to identify potential winnowing (Horton *et al.*, 1992; Hammarlund and Keen
343 1994). Both Platovo and Margaritovo are the basal beds of alluvial sequences, where reworking from
344 underlying deposits may be expected. At Platovo, the reworking of the opercula is supported by the
345 reworked small mammals, with redeposited early Calabrian small mammal material present in this
346 horizon (Tesakov *et al.*, 2007b).

347

348 The sediments from Semibalki 2 are correlated with the early Middle Pleistocene Cromerian complex
349 (MQR4-6). At this site the Cromerian deposits lie immediately on top of latest Calabrian estuarine
350 deposits ('Tamanian clays'), so there is potential for the opercula with higher D/L values to have been
351 reworked from these underlying deposits. The opercula with the highest D/Ls from Semibalki 2 yielded
352 values similar to the lowest from Semibalki 1 (Fig. 9), a horizon which is correlated with the latest Early
353 Pleistocene and MQR 7. This is therefore consistent with the interpretation that the high D/L value

354 opercula at Semibalki 2 are reworked from this lower layer. However there is considerable variability in
 355 the opercula D/L values at Semibalki 1, indicating significant reworking of the opercula through the
 356 sequence at this site (Fig. 9). Although there is no evidence of redeposition from the small mammal fauna,
 357 the reworking of the opercula is not inconsistent with the general site histor. The Semibalki 2 deposits
 358 form part of the large scale palaeo-Don river, with underlying lagoonal-estuarine deposits of the same
 359 large river, so reworking from older deposits due to river erosion is plausible.

360



361

362 Figure 9. FAA vs THAA D/Ls for Asx, Ala, Glx and Val for the intra-crystalline fraction of bithyniid
 363 opercula from Semibalki 1 and 2. N.B. axes do not start at 0.

364

365 A thick (~20 m) sequence at Stefanidinodar has yielded an early Middle Pleistocene small mammal

366 assemblage attributed to MQR4-6. The IcPD data from three of the bithyniid opercula are consistent with

367 this age attribution despite exhibiting a larger than expected range of values, but one falls within the
368 cluster of late Early Pleistocene material (Fig. 8). This suggests reworking, although this is otherwise not
369 evident from other palaeontological and lithological data.

370
371 The potentially higher potential for reworking of opercula versus other fauna is therefore important to
372 consider when interpreting age based on this method. However IcPD analyses on individual opercula
373 from single horizons could therefore provide a very useful indicator for assessing the integrity of the
374 geological history of fluvial formations.

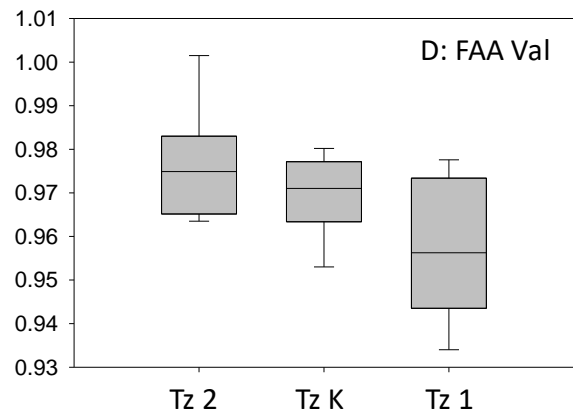
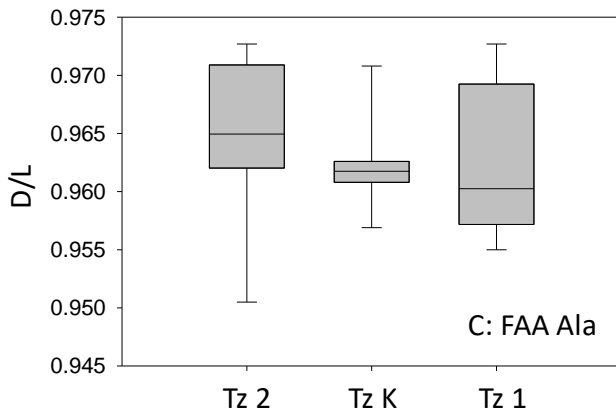
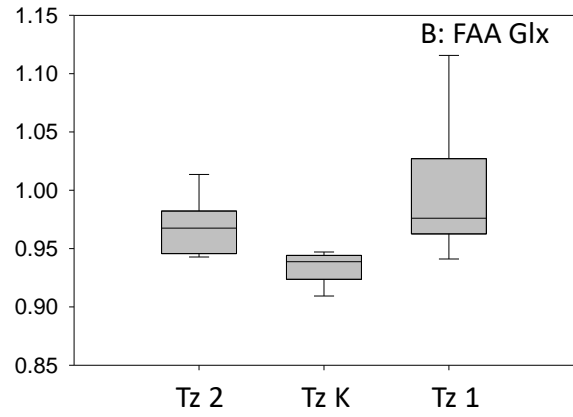
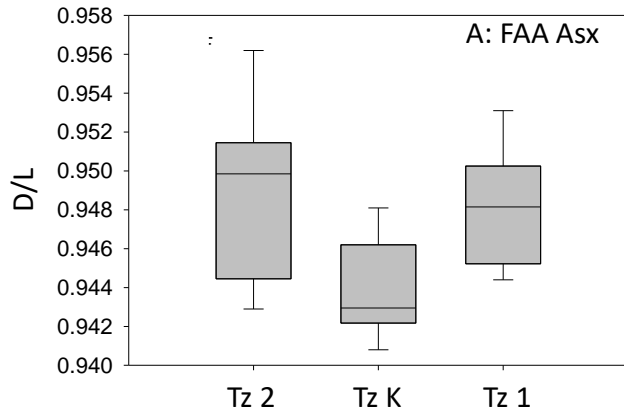
375

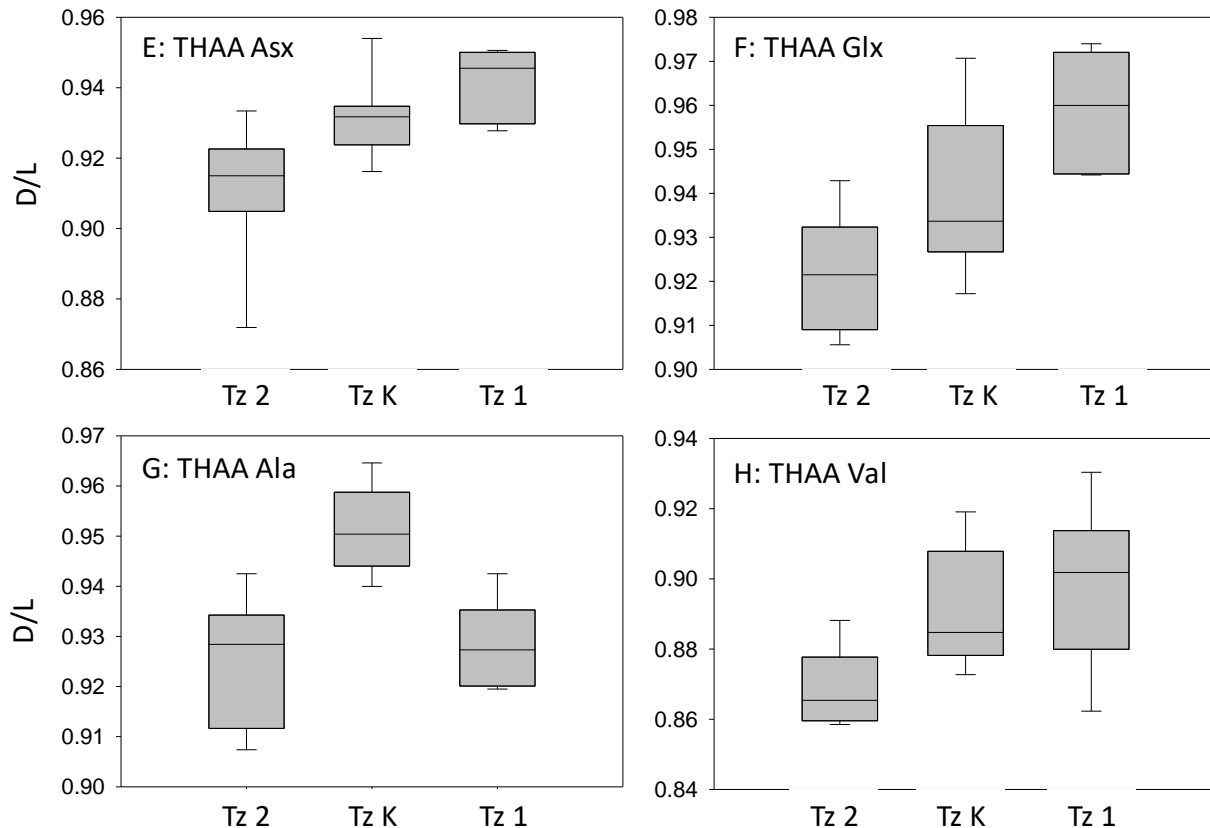
376 **3.6 Evidence of geothermal impact on IcPD at Tizdar**

377

378 Samples have been analysed from three stratigraphically superimposed horizons at Tizdar dating from the
379 Gelasian – Calabrian transition (~ 2 Ma). Tizdar 2, attributed to MQR10 overlies Tizdar K / Kermek
380 (MQR 10), which in turn overlies Tizdar 1 (MQR11). Intra-crystalline protein is clearly still present (Figs.
381 8a-d) but using FAA alone, the three horizons cannot be resolved (Fig. 10). The THAA for Asx, Glx and
382 Val do show increasing levels of racemisation through the sequence (Fig. 10), which indicates that there is
383 potential age discrimination, although the amino acids are all approaching equilibrium which may
384 preclude any differentiation. Application of the ultra-high pressure liquid chromatography (UHPLC)
385 method (Crisp, 2013), which is able to elute the slower racemising amino acids with baseline resolution, is
386 likely to improve the dating of samples of this age.

387





389

390 Figure 10. D/L values of amino acids from bithyniid opercula from three horizons at Tizdar: Tizdar 2
 391 (Tz2) overlies Tizdar Kermek (Tz K), which overlies Tizdar 1 (Tz 1). All amino acids are approaching
 392 equilibrium so the correct age order is only seen for three amino acids (THAA Asx, Glx and Val). For
 393 each sample, the box brackets the 25th and 75th percentiles. Within the box, the solid line indicates the
 394 median and the dashed line shows the mean, whereas the 10th and 90th percentiles are shown by lines
 395 below and above the boxes respectively. The results of each duplicate analysis are included in order to
 396 provide a statistically significant sample size
 397

398 The extent of the IcPD in the Tizdar samples is, however, higher than expected for their respective
 399 mammal zones (Figs. 7, 8a-d), showing greater racemisation than samples from the older Gelasian and
 400 Piacenzian sites. Reworking cannot be excluded, but it is less likely at Tizdar as it overlies predominantly
 401 marine deposits. However a possible explanation for this unusual situation may be related to the peculiar
 402 geological setting of this locality. Unlike all the other sites studied, the Tizdar sequence occurs in an area
 403 affected by active tectonics and mud volcanism, as demonstrated by tectonic tilting of the section and the
 404 occurrence of volcanic mud breccias that underlie and overlie the fossiliferous beds in this sequence.
 405 Occasional high-energy eruptions of mud volcanoes are a common feature of the Taman Peninsula

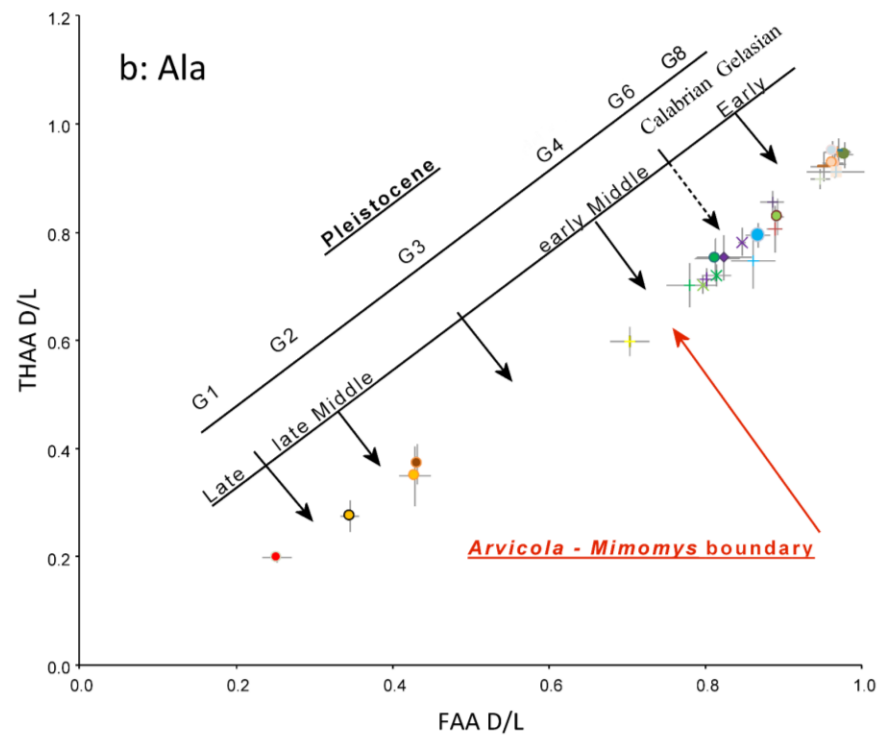
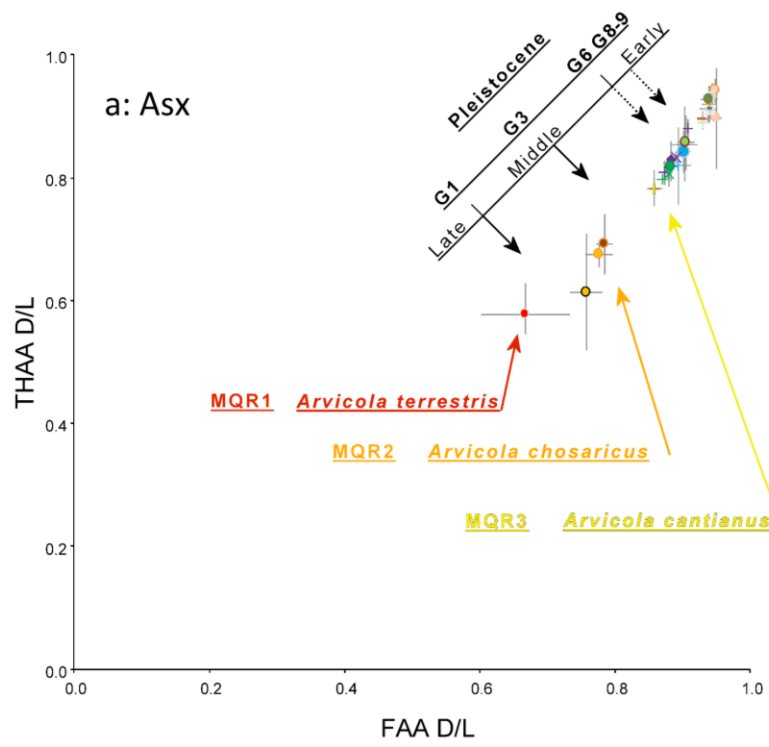
406 (Sobissevich *et al.*, 2008; Ovsyuchenko *et al.*, 2017). These eruptions reflect increased geothermal
407 activity, resulting in local explosions and burning of volcanic methane that may potentially involve
408 heating of the local sediments (Mukhtarov, 2003; Ershov *et al.*, 2015). These catastrophic eruptions
409 transport to the surface large volumes of hot mud. Thus, given the emplacement of the mud volcanic
410 sediment within this section (Fig. 4), the unexpectedly high IcPD levels could result from such post-
411 depositional heating. Little work has been undertaken on high temperature heating of opercula, but the
412 data obtained on ostrich eggshell (Crisp, 2013) show that heated eggshell tends to show characteristic
413 patterns of lower Glx D/L than expected for a given Asx D/L in the THAA fraction; heating experiments
414 on opercula may provide useful insights into this.

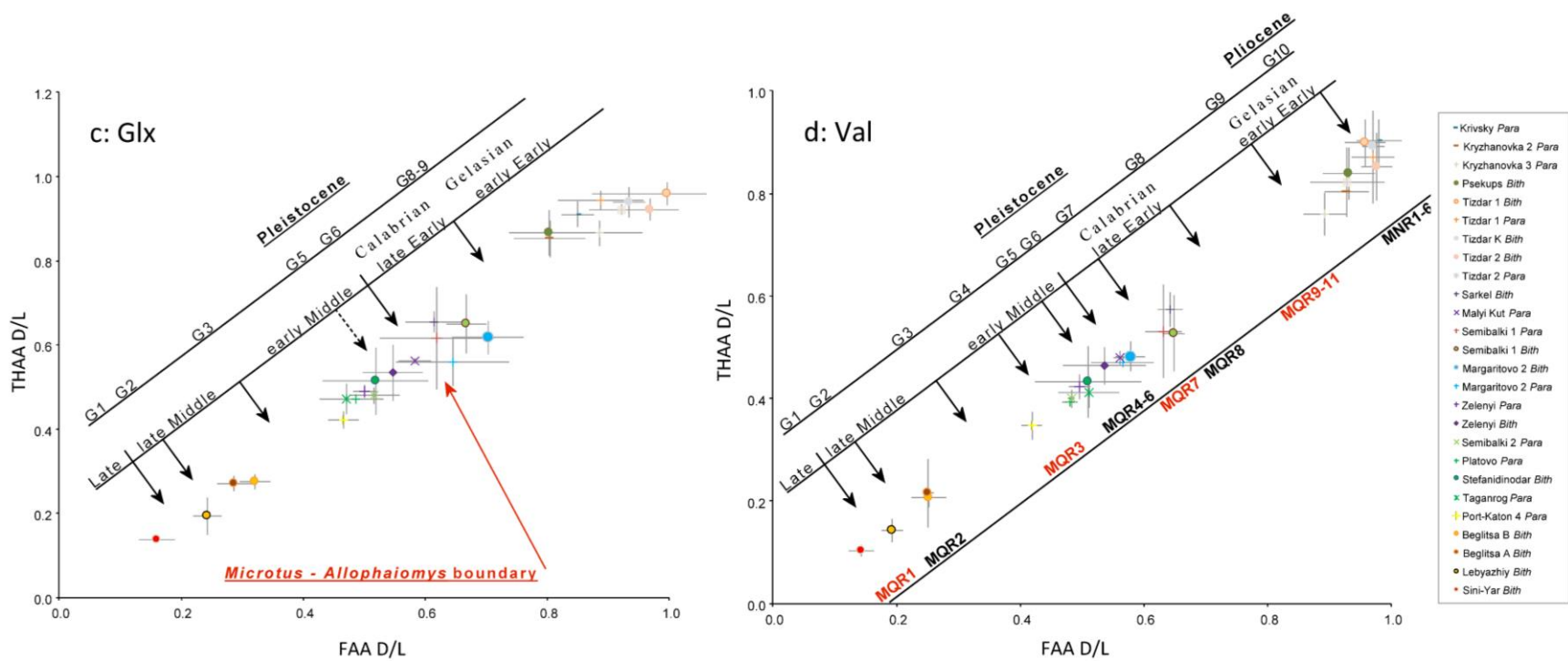
415

416 **3.7: IcPD-based aminostratigraphy of the Azov region**

417

418 The terrestrial mammalian record for south-east Europe is patchy and includes numerous isolated fossil
419 localities unevenly scattered throughout this large region. The current study is based on 20 analysed levels
420 from 16 reference sections (Fig. 4) from which the mammalian assemblages have previously been
421 attributed to the regional biozones (Vangengeim *et al.*, 2001; Tesakov, 2004). Due to the natural gaps in
422 the completeness of the geological record, these particular assemblages are distributed unevenly in time,
423 with some intervals over- or underrepresented. We therefore reviewed the aminostratigraphic sequence
424 (Figs. 8 and 11) paying attention to any breaks in its continuity, and compared this pattern to the known or
425 presumed gaps in the local biostratigraphical record. We designated any likely gaps in the
426 aminostratigraphic record as G1-G10; due to the differing levels of temporal resolution between the
427 amino acids, not all gaps are evident in all amino acids, but there is a consistent pattern in the dataset.





429

430

431 Figure 11. Site mean FAA vs THAA D/Ls for (a) Asx, (b) Ala, (c) Glx and (d) Val for the intra-crystalline fraction of bithyniid opercula from the
 432 Azov region, excluding samples identified as reworked. Error bars show two standard deviations about the mean for each site. Diagonal axes
 433 show how the amino acid data relate to the divisions of the Pleistocene and the East European Mammal zones (MQR/MNR zonation). G1-G10
 434 highlight likely gaps in the range of D/L values that correspond to breaks in the regional fossil record. Coloured arrows indicate important
 435 biostratigraphical events.

436

437

438 Aspartic acid / asparagine (Asx) is the fastest racemiser in our set and shows good closed-system
439 behaviour (Fig. 8a). Asx clearly resolves the Late Pleistocene, post-Eemian, fauna of Siniy Yar that
440 includes *Arvicola terrestris* (MQR1) from late Middle Pleistocene, pre-Eemian faunas that include less
441 advanced *Arvicola chosaricus* (MQR2), but as expected the temporal resolution is poor for older
442 deposits/samples including those of early Middle Pleistocene age (Fig. 11). Two apparent gaps in Asx
443 D/L data correspond to the early Late Pleistocene (G1) and mid-Middle Pleistocene (G3) time intervals
444 not represented in the Azov faunal sequence. Gaps between Middle and Early (G6) and within the Early
445 Pleistocene, i.e. Calabrian and Gelasian (G8-9) are less conspicuous. The largest gap in this record is
446 observed between the youngest studied site of Siniy Yar (MQR1, post-Eemian, possibly MIS 3, Tesakov
447 *et al.*, 2012) and modern samples (Penkman *et al.*, 2011). This would imply high potential resolution for
448 discriminating terminal Late Pleistocene and Holocene opercula.

449

450 Alanine (Ala) is a medium-rate racemiser and in our dataset enables good resolution back to the early
451 Middle Pleistocene, correlated with the Cromerian of NW Europe (Fig 11b). It is also able to separate out
452 the Calabrian from Gelasian - Calabrian transition. The most obvious gap is between late Middle
453 Pleistocene and the late Cromerian faunas (G3), suggesting potentially high resolution of the Ala amino-
454 chronometer for the mid Middle Pleistocene faunas in the region. Also conspicuous is the break within
455 early Middle Pleistocene cloud (G4) encompassing the *Arvicola/Mimomys* transition, a major
456 biostratigraphic boundary in continental Eurasia in the Middle Pleistocene (von Koenigswald and van
457 Kolfshoten, 1996; Maul *et al.*, 2000; Maul and Parfitt, 2010).

458

459 Glutamic acid / glutamine (Glx) is a slower racemiser providing better differentiation between the older
460 sites (Fig. 11c) than either Asx or Ala. More obvious gaps between clusters are apparent in the Glx D/L
461 values, which clearly highlights a hiatus between the Middle and Early Pleistocene, which corresponds to
462 the *Allophaiomys/Microtus* transition (MQR7). The higher Glx D/L values from Margaritovo 2 are

463 consistent with a late Calabrian age, with the site probably dating from the interval between the Brunhes-
464 Matuyama and the normally-magnetised event interpreted as the Jamarillo (Tesakov *et al.*, 2007b). Sarkel
465 (MQR8) has yielded a mid-Calabrian fauna, and is therefore older than Margaritovo 2 (MQR7), consistent
466 with its higher THAA Glx D/L values. An extended gap (G8-9) between the mid Calabrian and Gelasian
467 implies better resolution in this time interval. Kryzhanovka 2, with *Borsodia paehungarica paehungarica*,
468 is correlated with the earliest Gelasian and has higher FAA Glx D/L than the stratigraphically younger
469 Kryzhanovka 3, with the more advanced *B. p. cotlovinensis*, correlated with the mid-Gelasian. However
470 Glx D/L values are nearing equilibrium by this point, limiting its time-range beyond 2 Ma.

471
472 The latest Cromerian site Port-Katon 4 (MQR3) with *Arvicola* has a FAA Glx D/L similar to Cromerian
473 sites (MQR4-6) yielding the ancestral progenitor *Mimomys*. Margaritovo 2 (terminal Calabrian, MQR7)
474 has similar FAA D/L values to older, mid Calabrian clusters of Semibalki 1 and Sarkel (MQR8). The
475 relative difficulty of measuring FAA Glx results from the formation of the pyroglutamic acid lactam
476 (Wilson and Cannan, 1937). This cannot be derivitized and reduces the apparent concentration, which has
477 impacts on the accuracy of the FAA Glx D/L, as shown here by the FAA D/L Glx of Port-Katon 4 and
478 Margaritovo 2. However discrimination between these samples is possible using THAA Glx D/L, and
479 when comparing D/L Ala, Val, and even Asx. The clustering of the sites is therefore consistent with
480 biostratigraphical evidence. It can thus be concluded that in cases where anomalously high values of FAA
481 are seen compared to THAA in Glx, THAA D/L Glx provide the more accurate relative ages.

482
483 Valine (Val) is also a relatively slow racemiser, allowing better resolution for the older samples compared
484 to Asx, Ala, and Glx (Fig. 11d). The resolution of Val is consistently high in all parts of the chronological
485 sequence and it reveals the greatest numbers of discrete temporal breaks than any of the other amino acids
486 analysed here. As expected, Sarkel (MQR8) has higher FAA and THAA Val D/L than Margaritovo 2
487 (MQR7). The discontinuity in the Val D/L record between the Gelasian/Calabrian transition and the mid
488 Calabrian is reflected by faunal differences, because no assemblages attributed to MQR 9 are known from

489 the region. Tantalisingly the reworked samples from Margaritovo (see Section 3.5) fall within the MQR 9-
490 11 zone (Fig. 8d), indicating that a deposit of this age occurs in the vicinity.

491
492 In Val, the D/L data for the Gelasian sites Kryzhanovka 2 and 3 (MNR3 and MNR2) are very similar
493 which, although consistent with biostratigraphy, indicates a loss of resolution by this time. The
494 biostratigraphically younger site of Psekups (MNR1) also appears to be strongly racemised. It is therefore
495 possible to recognise that all these sites are significantly old, but discrimination between them presents a
496 challenge. The oldest site within the group, Krivsky (Piacenzian, between 3 - 2.5 Ma), also generally has
497 the highest D/L values, although within the range of other Gelasian sites (ca. 2.5 - 2 Ma). As the data from
498 Tizdar show anomalously high D/L values that appear to result from geothermal heating, they cannot be
499 used in the construction of the regional aminostratigraphy (see Section 3.6).

500
501 In summary, there are ten potential breaks (G1 –G10) between clusters of D/L values (Figs. 8 & 11): G1
502 (MQR1/2) occurs between the Late and Middle Pleistocene; G2 (within MQR2), between two late Middle
503 Pleistocene distributions; G3 (MQR2/MQR3), between late Middle Pleistocene and youngest Cromerian
504 record; G4 (MQR3/MQR4-6), between the younger and older Cromerian; G5 (MQR4-6/MQR7), between
505 late and earlier Cromerian levels; G6 (in-MQR7, only really evident in Glx), between early Middle and
506 late Early Pleistocene levels; G7 (MQR7/MQR8), between late Early and mid Early Pleistocene faunal
507 levels; G8 and G9 (MQR8/MQR9-11), between mid Early Pleistocene and the earliest Pleistocene
508 (Calabrian/Gelasian) distributions; and potentially G10 (MNR3/MNR5), between Late Pliocene and Early
509 Pleistocene (Piacenzian/Gelasian), although the Tizdar dataset is complex. Integrating this
510 aminostratigraphic dataset with the biostratigraphy of this well-studied region, we propose that these
511 breaks correspond to actual gaps (lack of deposits/localities) in the regional sequence, as a consequence of
512 local breaks in the continuity of the fossil record (non-deposition, erosion, etc.).

513
514 In summary, the increase in opercula IcpD is stratigraphically consistent with the East European Mammal

515 zonation. As the protein decomposition rate in a closed system depends on time and temperature, the
516 regional pattern of IcPD through time is controlled by the thermal history of that region (Miller *et al.*,
517 1999; Wehmiller *et al.*, 2000). Compared to the British aminostratigraphic sequence (Fig. 14 in Penkman
518 *et al.*, 2013), the IcPD values from bithyniid opercula in southern Eastern Europe are systematically
519 higher for a given time period, which is logical given the more southerly latitude.

520

521 **3.8: Comments on the regional biostratigraphy of southern Eastern Europe.**

522

523 Taking into account the different resolutions in different parts of the chronological sequence, the most
524 important feature of this aminostratigraphy is the reproducibility of the results using four amino acids, and
525 the striking fidelity of the aminostratigraphy in relation to the mammalian biostratigraphy. This enables
526 us to use the aminostratigraphic dataset (Fig. 11) to provide valuable insights into the nature of the
527 regional biostratigraphy.

528 The substantial gap between the early Middle Pleistocene (Cromerian) and late Middle Pleistocene D/L
529 values (Fig. 11) reflects a substantial stratigraphical hiatus from the interval spanning MIS 9-11, which
530 corresponds to the MQR3-MQR2 transition. Alluvial sites of this age are scarce in the region and not
531 represented in the analyses. Samples from the early Middle Pleistocene (Cromerian), yielding
532 mammalian faunas of the Tiraspol faunal complex (MQR 4-6), are well represented in the data set (7 out
533 of total 20). All belong to the palaeo-Don River Semibalki fluvial formation. Some samples show high
534 variability of D/L values within a single horizon, interpreted as the co-occurrence of both *in situ*
535 specimens (tight clusters) and a tail of reworked outliers (see Section 3.5). Both subclusters are divided by
536 G5, best seen in Glx and Val data (Fig. 8 c,d). The group forming the tail probably reflects a period close
537 to the Brunhes-Matuyama palaeomagnetic reversal that is not represented in the sections studied, and it is
538 likely that opercula from deposits of this period have been reworked by later fluvial activity.

539 The site of Malyi Kut, poorly characterised by a small mammal fauna, had been tentatively attributed to
540 the Calabrian mammal zones (MQR9-7). The aminostratigraphical evidence (Fig.8 b-d) suggests a

541 younger age in this range, possibly the early part of MQR7. Data from the Semibalki 1 site plot in the
542 same chronological position, although some of the specimens from here seem to be reworked from two
543 different Calabrian levels. The only reliable mid Calabrian level (MQR8) in our material is represented
544 by the homogeneous cluster of D/L values from Sarkel. Additional specimens that plot next to Sarkel
545 represent reworked material from latest Calabrian (MQR7) and Cromerian sites (MQR4-6).

546 The large gap in the early Calabrian (G8-9) would be occupied by mammal biozones MQR9-11. It is
547 remarkable that data from reworked bithyniid opercula from the neighbouring sites of Semibalki 1 and
548 Margaritovo 2 (both MQR7) plot in the gap (Fig. 8c-d). This indicates the former presence of early
549 Calabrian deposits on the southern shore of the Taganrog Gulf. The materials from Tizdar (MQR10-11)
550 that would have been expected to plot in G9 may be misplaced as a consequence of geothermal heating
551 (see Section 3.6), and imply that in geothermally active regions the aminostratigraphic technique should
552 be applied with caution.

553 The temporal resolution using IcPD in bithyniid opercula is poor for sites of Gelasian age. The data for
554 three Gelasian sites (Psekups, Kryzhanovka 3, and Kryzanovka 2) representing three mammal zones
555 during this interval (MNR1-2-3) show similar levels of protein breakdown, precluding finer temporal
556 resolution. The oldest site of Krivsky dating back to the Late Pliocene (mid Piacenzian, > 3 Ma, MNR5)
557 furnished opercula tending to show the highest racemization for Glx and Val, consistent with its greater
558 age. However these values fell within the higher end of the range for other Gelasian sites, and as all of the
559 amino acids reported in this study are nearing equilibrium at this point, so no further resolution is
560 currently possible using IcPD in opercula for this time interval.

561

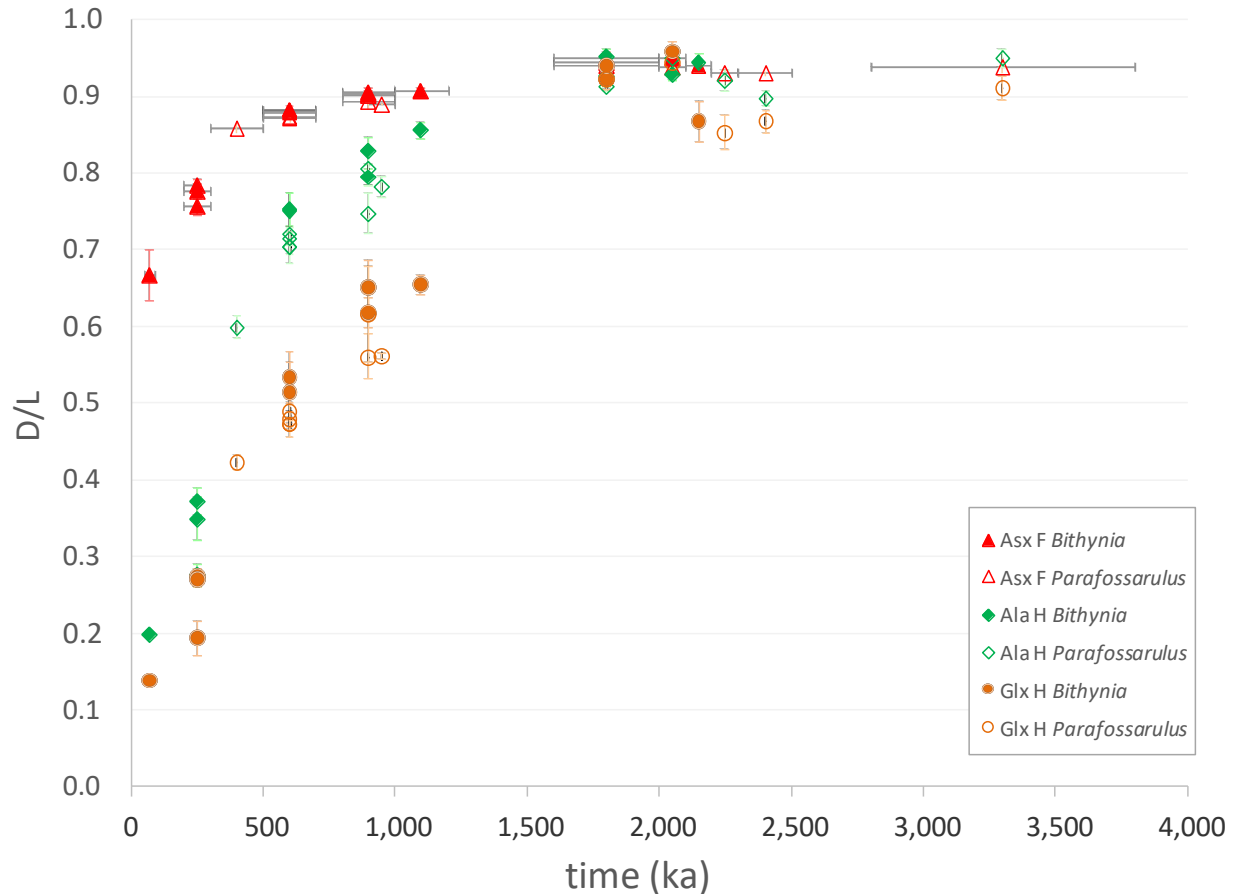
562 **4. Implications for Quaternary chronology and biostratigraphy of Europe.**

563

564 This study provides an example of how this synthetic regional chronology can be developed; combining
565 all available data and cross-testing the sequence, materials and regional geological history. The regional
566 mammal zones were defined from widely scattered sequences in the Azov/Black Sea region (Tesakov,

567 2004, Tesakov *et al.*, 2007), where only rarely do sediments yielding mammals attributable to
568 biostratigraphic zones occur in direct stratigraphical superposition. This is why the independent testing of
569 this system by opercula IcPD provides valuable age constraints. From the aminostratigraphical point of
570 view, following the first regional IcPD framework which was developed for Britain (Penkman *et al.*,
571 2011, 2013), this is the second large-scale application of opercula IcPD that has been undertaken, and is
572 the first in continental Europe. The high fidelity of the independently-constructed chronological sequences
573 of these fossil localities shows the important role aminostratigraphy can play in testing and providing
574 additional support to the standard integrated stratigraphy, and enables the stratigraphic extension to sites
575 where faunas are incomplete (Fig. 11 & 12). This provides a basis to develop regional chronologies for a
576 cross-European aminostratigraphy, enabling us to track IcPD behaviours across latitudes and temperature
577 zones. The Azov region was never covered by glacial ice, and periglacial conditions would only have
578 been present during the glacial stages of the Middle and Late Pleistocene (Velichko *et al.*, 2011), so more
579 data will illuminate the impacts of these differing depositional histories on the integrated effective
580 temperatures experienced by the opercula samples.

581 The reliable temporal range of the opercula IcPD in southern Eastern Europe extends to ~1.5-2 Ma (Fig.
582 12). For the Early Pleistocene / Late Pliocene, the resolution within current well-chromatographically
583 resolved amino acids is reaching its limit. However there is potential to extend this to other amino acids
584 using UHPLC technology (Crisp, 2013), which improves the chromatographic resolution of certain amino
585 acids as well as resolving addition amino acid D/L pairs. In addition, using other biominerals (such as the
586 hydroxyapatite of tooth enamel) where the racemisation of amino acids is slower (e.g. Dickinson *et al.*,
587 2019) will enable better resolution of Late Neogene samples from this region.



588
 589 Figure 12. Mean D/L values (Asx, Ala and Glx) for each site, excluding samples identified as reworked,
 590 from bithyniid opercula plotted against independent evidence of age. For simplicity, the x-error bars,
 591 indicating the current uncertainty on the age of the deposits, are shown for the Asx data. Y-error bars
 592 indicate two standard deviations about the mean for each site. *Bithynia* opercula are represented by closed
 593 symbols; *Parafossarulus* opercula by open symbols.
 594

595 Although the East European Mammal zonation was originally based on assemblages of small mammals
 596 from reference sites in the Azov Sea and Black Sea regions, it has subsequently been used to correlate
 597 Plio-Pleistocene sequences across much of Europe (Gromov, 1948; Rekovets and Nadachowski, 1995;
 598 Mayhew, 2015) and western Asia (Borodin *et al.*, 2019; van den Hoek Ostende *et al.*, 2015). It has been
 599 particularly important in dating critical sites in the early Paleolithic, and in estimating the magnitude of
 600 regional breaks in paleontological record (such as the late Calabrian ‘*Allophaiomys* gap’ in England; e.g.
 601 Preece *et al.*, 2020). The water vole lineage, incorporating the important *Mimomys/Arvicola* transition in
 602 the early Middle Pleistocene, has now been shown to exhibit exactly the same sequence of events and

603 relative chronology as seen in Western and Central Europe (Maul *et al.* 2000). The same is true for the
604 *Mammuthus* lineage, for which our opercula-based data are entirely consistent with the consecutive
605 occurrence of each named chrono-species within the Quaternary. This ground-truthing in the Azov region
606 therefore provides a useful mechanism for testing the assumptions that this East European Mammal
607 zonation scheme is applicable throughout Europe and western Asia (Mayhew, 2015). This new Azov
608 region aminostratigraphic dataset, combined with the British aminostratigraphy, therefore provides the
609 second foundation stone for development of a European-wide chronology.

610

611 *Data Availability:* All amino acid data from this study will be made available through the NOAA
612 repository upon publication: <ftp://ftp.ncdc.noaa.gov/pub/data/paleo/aar/>.

613

614 *Acknowledgements*

615

616 This study was financially supported by the joint grant of the Royal Society of London (IEC\R2\170162)
617 and the Russian Foundation of Basic Research, program no. 17-55-10013. Kirsty Penkman was
618 additionally supported by the Leverhulme Trust via PLP-2012-116. The support of the Calleva
619 Foundation to SAP is gratefully acknowledged. The study conforms to the state program of the scientific
620 research of the Geological Institute RAS no.0135-2019-0060. We thank Sheila Taylor and Kirsty High for
621 technical support. We also thank Vasily Lavrushin (Moscow) and Evgeny Shnyukov (Kiev) for discussion
622 on the thermal aspects of mud volcanism.

623

624 *Author contributions*

625 Roles of the authors: KP and AT led this study. AT coordinated the synthesis of the stratigraphic and
626 biochronological information on the paleontological record from the studied region; KP coordinated the
627 aminostratigraphic study. PF and VT provided data on the molluscan and large mammal fossil record in
628 southern Russia. TM provided materials on fossil molluscs from the Netherlands. RP, SP and MD

629 contributed to discussions on the correlations of the Russian and British fossil records. All authors were
630 involved in writing the manuscript.

631

632 *References:*

633 Agajanian, A.K. 2009. Pliocene-Pleistocene small mammals of the Russian Plain. Nauka, Moscow. 676 pp.
634 (Russian)

635 Alexandrova, L.P., 1976. Rodents of Anthropogene of European part of the USSR. Nauka, Moscow. 98
636 pp. (Russian)

637 Alexeeva, L.I., 1977. Theriofauna of Early Anthropogene of Eastern Europe. Nauka, Moscow, 214 pp.
638 (Russian).

639 Alexeeva, L.I., 1990. Upper Pleistocene theriofauna of Eastern Europe (large mammals). Moscow:
640 Nauka. 109 p. (Russian)

641 Annandale, T.N., 1924. Gastropoda. In: Annandale, T.N. and Prashad, B. Report on a small collection of
642 molluscs from the Chekiang Province of China. Proceedings of the Malacological Society of London 16,
643 27–49

644 Bajgusheva, V.S., Titov, V.V., Tesakov, A.S., 2001. The sequence of Plio-Pleistocene mammal faunas
645 from the south Russian Plain (the Azov Region). Bollettino della Societa Paleontologica Italiana 40 (2),
646 133–138.

647 Baygusheva, V., Titov V., 2012. The evolution of Eastern European meridionaloid elephants' dental
648 characteristics. Quaternary International 255, 206–216.

649 Baygusheva, V.S., Titov, V.V., Tesakov, A.S., Syromyatnikova, E.V., Kurshakov, S.V., Frolov, P.D.,
650 2014. Middle Pleistocene fauna of Veshenskaya (middle Don River, Rostov Region, Russia). In: Borodin,
651 A.V. et al. (Eds.), The Quaternary of the Urals: global trends and Pan-European Quaternary records:
652 International conference INQUA-SEQS 2014 (Ekaterinburg, Russia, September 10–16, 2014). Uralian
653 Federal University, Ekaterinburg, pp. 15–17.

654 Bell, C.J., Lundelius, jr., E.L., Barnosky, A., Graham, R.W., Lindsay, E.H., Ruez, jr., D.R., Semken, jr.,

655 H.A., Webb, S.D., Zakrzewski, R.J., 2004. The Blancan, Irvingtonian, and Rancholabrean mammal ages
656 In: Woodburne, M.O. (Ed.), Late Cretaceous and Cenozoic Mammals of North America: Biostratigraphy
657 and Geochronology. Columbia University Press, New York, 232–314.

658 Borodin, A.V., Strukova, T.V., Markova, E.A. 2019. Calabrian (Eopleistocene) micromammal assemblages
659 from the lacustrine and fluvial deposits of the Southern Trans-Urals and chronological position of some
660 regional stratigraphic units. Quaternary International 10.1016/j.quaint.2019.01.033.

661 Chegis, V., Zastrozhnov, A.S., Morozov, S.A., Tesakov, A.S., Kazanskiy, A.Yu., Frolov, P.D., Simakova,
662 A.N., Aleksandrova, G.N. 2017. New stratigraphic data on Pliocene Quaternary deposits from lower Don
663 region. Lavrushin et al. (Eds.) Materials of X all-Russia Congress for the study of Quaternary. Geos,
664 Moscow, 456–458. (Russian)

665 Chen, J., Yang, T., Matishov, G.G., Velichko, A.A., Zeng, B., He, Y., Shi, P., Fan, Zh., Titov, V.V.,
666 Borisova, O.K., Timireva, S.N., Konstantinov, E.A., Kononov, Yu.M., Kurbanov, R.N., Panin, P.G.,
667 Chubarov, I.G., 2018. A luminescence dating study of loess 14. Dodonovdeposits from the Beglitsa
668 section in the Sea of Azov, Russia. Quaternary International, 478, 27–37.

669 Cione, L.A., Tonni, E.P., 2005. Biostratigrafía basada en mamíferos del Cenozoico superior de la Región
670 Pampeana. In: Barrio R., Etcheverry R.O., Caballé M.F. & Llambías E. (Eds.): Geología y Recursos
671 Minerales de la provincia de Buenos Aires (Relatorio del XV Congreso geológico Argentino, La Plata,
672 11, 183–200.

673 Cohen, K.M., Gibbard, P.L., 2019. Global chronostratigraphical correlation table for the last 2.7 million
674 years, version 2019 QI-500. Quaternary International 500, 20–31.

675 Crisp, M.K., 2013. Amino acid racemization dating: method development using African ostrich (*Struthio*
676 *camelus*) eggshell. Unpublished PhD thesis, University of York.

677 Dickinson, M.R., Lister, A.M., Penkman, K.E.H., 2019. A new method for enamel amino acid
678 racemization dating: A closed system approach. Quaternary Geochronology 50, 29–46.

679 Dodonov, A.E., Tesakov, A.S., Titov, V.V., Inozemtsev, S.A., Simakova, A.N., Nikolskiy, P.A.,
680 Trubikhin, V.M., 2007. New data on the stratigraphy of Pliocene-Quaternary deposits of lower Don area:

681 sections along coasts of Tsymla Reservoir. Gladenkov Yu.B. (Ed.). Geological events of Neogene and
682 Quaternary of Russia: modern stratigraphic schemes and paleogeographic reconstructions. Geos, Moscow,
683 43–53. (Russian)

684 D-maps.com, free maps. <http://d-maps.com> (accessed May, 2017)

685 Ershov, V.V., Sobissevich, A.L., Puzich, I.N. 2015. Deep underground structure of mud volcanoes in
686 Taman according to experimental field studies and mathematical modeling. Geophysical Research 16(2),
687 69–76. (Russian, English abstract)

688 Fejfar, O., Heinrich, W.-D., Pevzner, M.A., Vangengeim, E.A., 1997. Late Cenozoic sequences of
689 mammalian sites in Eurasia: an updated correlation. Palaeogeography, Palaeoclimatology, Palaeoecology
690 133, 259–288.

691 Fejfar, O., Heinrich, W.-D. & Lindsay, E.H., 1998. Updating the Neogene rodent biochronology in
692 Europe. Mededelingen Nederlands Instituut voor Toegepaste Geowetenschappen TNO 60, 533–554.

693 Flynn, L., Wu, W.-Y., 2017. Chapter 16. Dynamic Small Mammal Assemblages of Yushe Basin In:
694 Flynn, L., Wu, Wen-Yu (Eds.), Late Cenozoic Yushe Basin, Shanxi Province, China: Geology and Fossil
695 Mammals. Volume II: Small Mammal Fossils of Yushe Basin Springer Science+Business Media,
696 Dordrecht, 205–215.

697 Freudenthal, M., Meijer, T., van der Meulen, A. 1976. Preliminary report on a field campaign in the
698 continental Pleistocene of Tegelen (The Netherlands). Scripta Geologica 34, 1–27.

699 Girotti, O. 1972. Il genere *Neumayria* Stefani 1877 (Gastropoda, Prosobranchia). Geologica Romana, 11:
700 115–136.

701 Gittenberger, E., Janssen, A.W., Kuijper, W.J., Kuiper, J.G.J., Meijer, T., van der Velde, G., de Vries,
702 J.N., 1998. De Nederlandse zoetwatermollusken. Recente en fossiele weekdieren uit zoet en brak water.
703 Nederlandse Fauna 2. Nationaal Natuurhistorisch Museum Naturalis, KNNV Uitgeverij & EIS-Nederland,
704 Leiden.

705 Gromov, V.I., 1948. Paleontological and archaeological basis of stratigraphy of continental deposits of
706 USSR territory (Mammals, Palaeolithic). Trudy instituta geologicheskikh nauk, Ser. geology 64 (17), pp.

707 1–520. (Russian)

708 Guérin, C., 1982. Première biozonation du Pléistocène européen, principal résultat biostratigraphique de
709 l'étude des Rhinocerotidae (Mammalia, Perissodactyla) du Miocène terminal au Pléistocène supérieur
710 d'Europe occidentale. *Geobios* 15(4), 593–598.

711 Hammarlund, D., Keen D.H. 1994. A late Weichselian stable isotope and Molluscan Stratigraphy from
712 Southern Sweden. *GFF* 116(4), 235–248.

713 Hill, R.L., 1965. Hydrolysis of proteins. *Advances in Protein Chemistry* 20, 37-107

714 Horáček, I., Ložek, V. 1988. Paleozoology and the Mid-European Quaternary past: scope of the approach
715 and selected results. *Rozpravy Československé Akademie Věd, Řada matematických a přírodních věd*, 98,
716 1–102.

717 Horton, A., Keen, D.H., Field, M.H., Robinson, J.E., Coope, G.R., Carrant, A.P., Graham, D.K., Green,
718 C.P. & Phillips, L.M., 1992: The Hoxnian Interglacial deposits at Woodston, Peterborough. *Philosophical*
719 *Transactions of the Royal Society of London B*338, 131–164.

720 Iossifova, Yu.I., Semenov, V.V., 1998. Climate-stratigraphy of the Pre-Tiglian-Bavelian analogues in
721 Central Russia (the Don drainage basin) *Mededelingen Nederlands Instituut voor Toegepaste*
722 *Geowetenschappen TNO* 60, 327–338.

723 Kholmovoi. G.V. 2003. Neogene-Quaternary alluvium and natural resources in the basin of the Upper
724 Don River. Voronezh State University, Voronezh, 97 pp. (Russian)

725 Kosnik, M.A., Kaufman, D.S., 2008. Identifying outliers and assessing the accuracy of amino acid
726 racemization measurements for geochronology: II . Data screening. *Quaternary Geochronology* 3, 328–
727 341.

728 Krasnenkov, R.V., Kazantseva, N.E. 1993. Discovery of early Dnieper alluvium in terraces of the Upper
729 Don River. *Bull. Interdepartmental Stratigraphic Comm. of Center and South of Russian Platform* 2, 153-
730 162. (Russian)

731 Kretzoi, M. 1987. Remarks on the correlation between European and Asian Late Cenozoic local
732 biostratigraphies. *Vertebrata Palasiatica*, 25, 145–157.

733 Krijgsman, W., Tesakov, A., Yanina, T., Lazarev, S., Danukalova, G., Van Baak, C. G. C., Agustí, J.,
734 Alçiçek, M.C., Aliyeva, E., Bista, D., Bruch, A., Büyükmeriç, Y., Bukhsianidze, M., Flecker, R., Frolov,
735 P., Hoyle, T.M., Jorissen, E.L., Kirscher, U., Koriche, S.A., Kroonenberg, S.B., Lordkipanidze, D., Oms,
736 O., Rausch, L., Singarayer, J., Stoica, M., van de Velde, S., Titov, V.V., Wesselingh, F.P., 2019.
737 Quaternary time scales for the Pontocaspian domain: Interbasinal connectivity and faunal evolution.
738 *Earth-Science Reviews* 188, 1-40. doi:10.1016/j.earscirev.2018.10.013
739 Lewis, S.G., Parfitt, S.A., Preece, R.C., Sinclair, J., Coope, G.R., Field, M.H., Maher, B., Scaife, R.G.,
740 Whittaker, J.E. 2004. Age and palaeoenvironmental setting of the Pleistocene vertebrate fauna at Norton
741 Subcourse, Norfolk. In: Schreve, D.C. (ed.) *The Quaternary mammals of southern and eastern England.*
742 *QRA/Euromam Field Guide*, p 5-17.
743 Lisiecki, L.E., Raymo, M.E., 2005. A Pliocene-Pleistocene stack of 57 globally distributed benthic $d^{18}O$
744 records. *Paleoceanography* 20, PA1003.
745 Lowe, J.J., Bronk Ramsey, C., Housley, R.A., Lane, C.S., Tomlinson, E.L., RESET Team & RESET
746 Associates, 2015. The RESET project: constructing a European tephra lattice for refined synchronisation
747 of environmental and archaeological events during the last c. 100 ka. *Quaternary Science Reviews* 118, 1–
748 17.
749 Markova, A.K. 1982. Pleistocene rodents of the Russian Plain. Nauka, Moscow (Russian).
750 Markova, A.K. 1990. The sequence of Early Pleistocene small-mammal faunas from the South Russian
751 Plain. *Quartärpaläontologie* 8, 131–151.
752 Markova, A.K. 2005. Eastern European rodent (Rodentia, mammalia) faunas from the Early–Middle
753 Pleistocene transition. *Quaternary International* 131, 71–77.
754 Markova, A.K. 2007. Pleistocene mammal faunas of Eastern Europe. *Quaternary International* 160, 100–
755 111.
756 Markova, A. K., Vislobokova, I. A. 2016. Mammal faunas in Europe at the end of the Early – Beginning
757 of the Middle Pleistocene. *Quaternary International*, 420, 363–377.
758 Maul, L., Parfitt, S., 2010. Micromammals from the 1995 Mammoth Excavation at West Runton, Norfolk,

759 UK: Morphometric data, biostratigraphy and taxonomic reappraisal. *Quaternary International* 228, 91–
760 115.

761 Maul, L., Rekovets, L.I., Heinrich, W.-D., Keller, T., Storch, G., 2000. *Arvicola mosbachensis*
762 (Schmidtgen 1911) of Mosbach 2: A basic sample for the early evolution of the genus and a reference for
763 further biostratigraphical studies. *Senckenbergiana lethaea* 80(1), 129–147.

764 Mayhew, D.F. 2012. Revision of the fossil vole assemblage (Mammalia, Rodentia, Arvicolidae) from
765 Pleistocene deposits at Kisláng, Hungary. *Palaeontology* 55(1), 11–29.

766 Mayhew, D.F. 2015. Revised biostratigraphic scheme for the Early Pleistocene of the UK based on
767 arvicolids (Mammalia, Rodentia). *Geological Journal*, 50, 246–256.

768 Meijer, T. 1974. Aantekeningen over de Bithyniidae (Gastropoda, Streptoneura) in het Nederlandse
769 Kwartair. *Mededelingen van de Werkgroep voor Tertiaire en Kwartaire Geologie* 11(4), 149–171.

770 Meijer, T. 1986. Non-marine Mollusc biozonation of Quaternary deposits in the Netherlands. –
771 *Proceedings 8th International Malacological Congress, Budapest, 1983*, 161–163.

772 Meijer, T. 1989. Notes on Quaternary freshwater mollusca of the Netherlands, with descriptions of some
773 new species. *Mededelingen van de Werkgroep voor Tertiaire en Kwartaire Geologie*, 26(4), 145–181.

774 Mein, P., 1990. Updating of MN zones. In E.H. Lindsay, V. Fahlbusch, P. Mein (ed.), *NATO symp.*
775 *European Neogene Mammal Chronology*. Plenum Press Ed., New York, 73–90.

776 Miller, G.H., Magee, J.W., Johnson, B.J., Fogel, M.L., Spooner, M.A., McCulloch, M.T., Ayliffe, L.K.,
777 1999. Pleistocene of *Genyornis newtoni*: human impact on Australian megafauna. *Science* 283, 205–208

778 Mukhtarov, A. 2003. Geothermal Energy Discharge from Mud Volcano Channel. *AAPG Annual Meeting*,
779 May 11–14, 2003, Salt Lake City, Utah. *AAPG Search and Discovery*, Article #90013©2003, 1–7.

780 Natural Earth. Free vector and raster map data: <http://naturalearthdata.com> (accessed November, 2019)

781 Nesin, V.A., Nadachowski, A. 2001. Late Miocene and Pliocene small mammal faunas (Insectivora,
782 Lagomorpha, Rodentia) of Southeastern Europe. *Acta Zoologica Cracoviensia* 44(2), 107–135.

783 Nikolskiy, P.A., Titov, V.V., Tesakov, A.S., Foronova, I.V., Baygusheva, V.S. 2014. Early Biharian
784 *Archidiskodon meridionalis* (Nesti, 1825) from Sarkel (Lower Don area, southern European Russia) and

785 associated small mammals. *Scientific Annals*, School of Geology, Aristotle University of Thessaloniki,
786 Greece. VIth International Conference on Mammoths and their Relatives, Grevena - Siatista. Special
787 Volume 102,142.

788 Nomade, S., Pastre, J.F., Guillou, H., Faure, M., Guérin, C., Delson, Eric, Debard, E., Voinchet, P.,
789 Messager, E., 2014. $^{40}\text{Ar}/^{39}\text{Ar}$ constraints on some French landmark Late Pliocene to Early Pleistocene
790 large mammalian paleofaunas: Paleoenvironmental and paleoecological implications. *Quaternary*
791 *Geochronology* 21, 2–15.

792 Ovsyuchenko, A.N., Sobissevich, A.L., Sysolin, A.I., 2017. On the relationship between recent tectonic
793 processes and mud volcanism by the example of Mt. Karabetov, Taman Peninsula. *Izvestiya. Physics of*
794 *the Solid Earth*, 53(4), 606–617.

795 Penkman, K.E.H., Preece, R.C., Keen, D.H., Maddy, D., Schreve, D.C., Collins, M.J., 2007. Testing the
796 aminostratigraphy of fluvial archives: the evidence from intra-crystalline proteins within freshwater
797 shells. *Quaternary Science Reviews* 26, 2958–2969.

798 Penkman, K.E.H., Kaufman, D.S., Maddy, D., Collins, M.J., 2008. Closed-system behaviour of the
799 intracrystalline fraction of amino acids in mollusc shells. *Quaternary Geochronology*, 3, 2–25.

800 Penkman, K.E.H., Preece, R.C., Keen, D.H., Collins, M.J., 2010. Amino acid geochronology of the type
801 Cromerian of West Runton, Norfolk, UK. *Quaternary International* 228, 25–37.

802 Penkman, K.E.H., Preece, R.C., Bridgland, D.R., Keen, D.H., Meijer, T., Parfitt, S.A., White, T.S.,
803 Collins, M.J., 2011. A chronological framework for the British Quaternary based on *Bithynia* opercula.
804 *Nature*, 476, 446-449.

805 Penkman, K.E.H., Preece, R.C., Bridgland, D.R., Keen, D.H., Meijer, T., Parfitt, S.A., White, T.S.,
806 Collins, M.J., 2013. An aminostratigraphy for the British Quaternary based on *Bithynia* opercula.
807 *Quaternary Science Reviews*, 61, 111–134.

808 Pilipenko, O.V., Trubikhin, V.M., Gribov, S.K. 2015. Petro- and paleomagnetism of the Malyi Kut Lower
809 Neo-Pleistocene marine deposits (Krasnodar Krai). *Geomagnetism and Aeronomy*, 55(3), 410–420.

810 Pogoda i klimat [Weather and climate] website, <http://www.pogodaiklimat.ru>, accessed May 2020.

811 Powell, J., Collins, M.J., Cussens, J., MacLeod, N., Penkman, K.E.H., 2013. Results from an amino acid
812 racemization inter-laboratory proficiency study; design and performance evaluation. *Quaternary*
813 *Geochronology* 16, 183-197.

814 Preece, R.C., 1990. The occurrence of the genus *Neumayria* (Gastropoda: Bithyniidae) in the British
815 Lower Pleistocene. *Journal of Conchology*, 33, 291–293.

816 Preece, R.C., Penkman, K.E.H., 2005. New faunal analyses and amino acid dating of the Lower
817 Palaeolithic site at East Farm, Barnham, Suffolk. *Proceedings of the Geologists' Association* 116, 363–
818 377.

819 Preece, R.C. Meijer, T., Penkman, K.E.H., Demarchi, B., Mayhew, D.F., Parfitt, S.A. 2020. The
820 palaeontology and dating of the 'Weybourne Crag', an important marker horizon in the Early Pleistocene
821 of the southern North Sea basin. *Quaternary Science Reviews* 236, 106177

822 Rekovets, L.I., Nadachowski, A., 1995. Pleistocene voles (Arvicolidae) of the Ukraine. *Paleontologia i*
823 *Evolucio* 28-29, 145–245.

824 Rook, L., Martínez-Navarro, B., 2010. Villafranchian: The long story of a Plio-Pleistocene European
825 large mammal biochronologic unit. *Quaternary International* 219, 134–144.

826 Sanko, A.F. 2007 *Quaternary freshwater molluscs from Belarus and neighbouring regions of Russia,*
827 *Lithuania, Poland (Field Guide).* Institute of Geochemistry and Geophysics National Academy of
828 *Sciences, Belarus (In Russian)*

829 Shchelinsky, V.E., Gurova, M., Tesakov, A.S., Titov, V.V., Frolov, P.D., Simakova, A.N., 2016. The
830 Early Pleistocene site of Kermek in western Ciscaucasia (southern Russia): Stratigraphy, biotic record and
831 lithic industry (preliminary results). *Quaternary International*, 393, 51–69.

832 Sobissevich, A.L., Gorbatikov, A.V., Ovsyuchenko, A.N., 2008. Deep structure of the Mt. Karabetov mud
833 volcano. *Doklady Earth Sciences*, 422(1), 1181–1185.

834 Tesakov, A.S., 2004. *Biostratigraphy of Middle Pliocene – Eopleistocene of Eastern Europe (Based on*
835 *Small Mammals).* Nauka, Moscow. (Russian)

836 Tesakov, A.S. 2016. Early Middle Pleistocene *Ellobius* (Rodentia, Cricetidae, Arvicolinae) from

837 Armenia. *Russian Journal of Theriology* 15, 151–158.

838 Tesakov, A.S., Vangengeim, E.A., Pevzner, M.A. 2007a. Arvicolid zonation of continental Pliocene of
839 East Europe. *Courier Forschungsinstitut Senckenberg* 259, 227–236.

840 Tesakov, A.S., Dodonov, A.E., Titov, V.V., Trubikhin, V.M., 2007b. Plio-Pleistocene geological record
841 and small mammal faunas, eastern shore of the Azov Sea, Southern European Russia. *Quaternary*
842 *International* 160, 57–69.

843 Tesakov, A.S., Simakova, A.N., Frolov, P.D., Titov, V.V., 2012. Biostratigraphy of Late Pleistocene
844 deposits of the section Sinii Yar in the lower course of the Severskii Donets River. *Vestnik of the*
845 *Southern Scientific Centre RAS*, 8 (4): 58–65. (Russian)

846 Tesakov, A.S., Titov, V.V., Sotnikova, M.V., Bondarev, A.A., Simakova, A.N., Frolov, P.D., 2017.
847 Revised Quaternary biochronological scheme of eastern Europe and Western Asia. In: Lavrushin, Yu.A.
848 (Ed.), *Materials of the Xth all-Russia conference on the study of Quaternary*. Geos, Moscow. 422–424.
849 (Russian)

850 Tesakov, A.S., Simakova, A.N., Frolov, P.D., Sytchevskaya, E.K., Syromyatnikova, E.V., Foronova, I.V.,
851 Shalaeva, E.A., Trifonov, V.G. 2019a. Early-Middle Pleistocene environmental and biotic transition in
852 north-western Armenia, southern Caucasus. *Palaeontologia Electronica* 22.2.25A 1–39.
853 doi.org/10.26879/916

854 Tesakov, A.S., Guydalenok, O.V., Sokolov, S.A., Frolov, P.D., Trifonov V.G., Simakova, A.N.,
855 Latyshev, A.V., Titov, V.V., Shchelinsky, V.E., 2019b. Tectonics of Pleistocene deposits in the Northeast
856 of Taman Peninsula, South Azov Sea Region. *Geotectonics*, 53(5), 548–568.

857 Titov, V.V., 2008. Late Pliocene large mammals from Northeastern Sea of Azov Region. SSC RAS
858 Publishing, Rostov-on-Don. (Russian, English summary).

859 Topachevsky, V.A., Scorik, A.F., Rekovets, L.I., 1987. Rodents of the Upper Neogene and Early
860 Anthropogene deposits of the Khadjibei Lagoon, Naukova Dumka, Kiev.

861 Topachevsky, V.A., Nesin, V.A., Topachevsky, I.V., 1998. Biozonal microtheriological scheme
862 (stratigraphic distribution of small mammals, Insectivora, Lagomorpha, Rodentia) of the Neogene of the

863 northern part of the Eastern Paratethys. Vestnik Zoologii 32 (1–2), 76–87. (Russian)

864 van den Hoek Ostende, L.W., Diepeveen, F., Tesakov, A.S., Saraç, G., Mayhew, D.F., Alçiçek, M.C.,
865 2015. On the brink: micromammals from the latest Villanyian from Biçakçi (Anatolia). Geological
866 Journal 50(3), 230–245.

867 Vangengeim, E.A., Pevzner, M.A., Tesakov, A.S., 2001. Zonal subdivisions of the Quaternary in Eastern
868 Europe based on small mammals. Stratigraphy. Geological Correlation 9 (3), 280–292.

869 Velichko, A.A., Faustova, M.A., Pisareva, V.V., Gribchenko, Yu.N., Sudakova, N.G., Lavrentiev, N.V.,
870 2011. Chapter 26 - glaciations of the East European Plain: Distribution and Chronology. In: Ehlers, J.,
871 Gibbard, P.L., Hughes, P.D. (Eds.), Developments in Quaternary Sciences 15. pp. 337–359. doi:
872 10.1016/B978-0444-53447-7.00026-X

873 von Koenigswald, W., van Kolfschoten, T., 1996. The *Mimomys* – *Arvicola* boundary and the enamel
874 thickness quotient (SDQ) of *Arvicola* as stratigraphic markers in the Middle Pleistocene. In: Turner, C.
875 (Ed.), The early Middle Pleistocene in Europe. Balkema, Rotterdam, pp. 211–226.

876 Walsh, S.L., 1998. Fossil datum and paleobiological event terms, paleostratigraphy,
877 chronostratigraphy, and the definition of Land Mammal “Age” boundaries. Journal of Vertebrate
878 Paleontology 18, 150–179.

879 Wehmiller, J.F., Stecher, H.A., York, L.L., Friedman, I., 2000. The thermal environment of fossils:
880 effective ground temperatures at aminostratigraphic sites on the U.S. Atlantic Coastal Plain. In:
881 Goodfriend, G.A., Collins, M.J., Fogel, M.L., Macko, S.A., Wehmiller, J.F. (Eds.), Perspectives in Amino
882 Acid and Protein Geochemistry. Oxford University Press, Oxford, pp. 219–250.

883 Wilke, T., Haase, M., Hershler, R., Liu, H.-P., Misof, B., Ponder, W., 2013. Pushing short DNA
884 fragments to the limit: Phylogenetic relationships of “hydrobioid” gastropods (Caenogastropoda:
885 Rissooidea). Molecular Phylogenetics and Evolution 66(3), 715–736.

886 Williams, K.M., Smith, G.G., 1977. A critical evaluation of the application of amino acid racemization to
887 geochronology and geothermometry. Orig. Life 8, 91–144.

888 Wilson, H., Cannan, R.K., 1937. The glutamic acid-pyrrolidonecarboxylic acid system. Journal of

889 Biological Chemistry 119, 309-331.

890 Zagwijn, W.H., 1985. An outline of the Quaternary stratigraphy of The Netherlands. *Geologie en Mijnbouw*, 64,
891 17–24.

892 Zastrozhnov, A.S., Danukalova, G.A., Golovachev, M.V., Titov, V.V., Tesakov, A.S., Simakova , A.N.,
893 Osipova, E.M., Trofimova, S.S., Zynoviev, E.V., Kurmanov, R.G., 2018. Singil deposits in the
894 Quaternary Scheme of the Lower Volga Region: New Data. *Stratigraphy and Geological Correlation* 26,
895 647–685.

896 Zatravkin, M.N., Dovgalev, A.S., Starobogatov, Ya.I., 1989. Molluscs of the genus *Parafossarulus*
897 (Bithyniidae, Gastropoda) in fauna of the USSR and their role as intermediate hosts of the trematode
898 *Clonorchis sinensis* (Cobbold, 1857). *Byulleten' Moskovskogo Obshchestva Ispytateley Prirody, otdel*
899 *biologicheskii* 94(5), 74–78. (Russian).

900